2018

Nonlinearity Modelling and Mitigation for LED Communications

Weikang Zhao
University of Wollongong

UNIVERSITY OF WOLLONGONG

Nonlinearity Modelling and Mitigation for LED Communications

Weikang Zhao

This thesis is presented as part of the requirements for the conferral of the degree:

Doctor of Philosophy

The University of Wollongong

School of School of Electrical, Computer and Telecommunications Engineering

July 2018

Declaration

I, Weikang Zhao, declare that this thesis submitted in partial fulfilment of the requirements for the conferral of the degree Doctor of Philosophy, from the University of Wollongong, is wholly my own work unless otherwise referenced or acknowledged. This document has not been submitted for qualifications at any other academic institution.

Weikang Zhao

October 23, 2018

Abstract

In recent years, light-emitting diodes (LEDs) technology, known as "Green Illumination", is growing rapidly. LED communications, or visible light communications is a promising field and is getting more and more research focus. LED is the major source of nonlinearity in LED communications, and the nonlinearity needs to be modelled effectively and thereby mitigated through pre-distortion or post-distortion to avoid severe degradation of communication performance.

The primary objectives of this thesis are to develop effective and efficient LED nonlinearity modelling and proper nonlinearity mitigation as well as signal detection techniques to mitigate the nonlinear and inter-symbol interference (ISI) distortions in LED communications.

Memory polynomial is often used for LED nonlinearity modelling and mitigation in the literature. However, the estimation of memory polynomial coefficients suffers from numerical instability, resulting in inaccurate modelling and poor performance in nonlinearity mitigation. Firstly, we focus on LED nonlinearity modelling and mitigation using memory polynomials. To solve the above numerical instability problem, we propose an alternative LED nonlinearity modelling technique based on orthogonal polynomials. For the first time, we develop a special set of orthogonal polynomial basis for LED communications with pulse amplitude modulation (PAM) signalling for LED nonlinear system

modelling. Due to the use of the orthogonal polynomials, the new basis matrix for the nonlinear model is quasi-orthogonal, which avoids the numerical instability problem during the estimation of the polynomial coefficients, and leads to low complexity and accurate LED nonlinearity modelling. Furthermore, a pre-distorter is employed to mitigate the LED nonlinearity. Simulations show that the proposed technique significantly outperforms the conventional memory polynomial based techniques.

Secondly, another challenge in indoor LED communications is that multipath dispersion can lead to ISI at high data rates. We extend our work on orthogonal polynomial based LED modelling technique and consider both the LED nonlinearity and ISI distortions due to LED memory effect and multipath dispersion. A joint estimation approach to LED nonlinearity and composite ISI channel based on orthogonal polynomial technique is proposed. Then, we design a receiver which consists of three modules, i.e., a nonlinearity and composite channel estimator, a frequency domain equalization (FDE) equalizer and a nonlinearity mitigator. For the first time, both ISI optical channel and LED nonlinearity with memory effects are jointly estimated and mitigated. Simulations show that the proposed technique can effectively handle the LED nonlinearity and ISI distortion.

Lastly, with effective LED nonlinearity modelling technique developed, we consider iterative nonlinearity mitigation and decoding in a coded LED communication system to boost the system performance. We develop a novel iterative receiver, which consists of a soft-in-soft-out (SISO) post-distorter and a SISO decoder. The SISO post-distorter is combined with a demapper to handle the distortion of LED nonlinearity and ISI, which works with a SISO decoder iteratively by exchanging log-likelihood ratios (LLRs) of the coded bits at the receiver. It is very different from the conventional post-distorters as

explicit polynomial inversion is not required, thereby avoiding the impact of imperfect polynomial inversion and the generation of colour noises. Simulations show that by taking advantage of the iterative processing between the SISO post-distorter and SISO decoder, remarkable performance gain can be achieved compared to the conventional techniques. In addition, the iterative receiver converges very fast.

Acknowledgments

I would like to take this opportunity to express my sincere thanks to all the people who helped me during my PhD studies.

Firstly, I would like to express my deepest gratitude to my principle supervisor, Dr. Qinghua Guo, for his patience, encouragement and guidance throughout my PhD career. Without his invaluable suggestions, insights and endless support, I could not have completed my dissertation. My grateful thanks also go to my co-supervisors, Dr. Jun Tong and Prof. Jiangtao Xi for their helpful suggestions and encouragements. I would also like to thank A/Prof. Yanguang Yu for her help and guidance.

My deepest thanks go to my friends and group-mates, Xiaochen He, Zichen Wang, Ying Liu, Dawei Gao, Yiwen Mao, Yiwei Zhang, Chengpu Duan, Jiayi Yang, Yuewen Zhu, Tianle Liu, Ke Lin, Bin Liu for their invaluable help and constructive discussions.

I would like to extend my thanks to all the staffs of the School of Electrical, Computer and Telecommunications Engineering for their professional help and supports.

Finally, I wish to express my deepest gratitude and love to my parents for their understanding, unconditional love and support throughout my life.

Author Publications

1. Weikang Zhao, Qinghua Guo, Jun Tong, Jiangtao Xi, Yanguang Yu, Pingjuan Niu and Xiaohong Sun, "Orthogonal polynomial-based nonlinearity modeling and mitigation for LED communications," *IEEE Photonics Journal*, vol.8, no.4, pp.1-12, August, 2016.

2. Weikang Zhao, Qinghua Guo, Jun Tong, Jiangtao Xi, Yanguang Yu and Pingjuan Niu, "Frequency Domain Equalization and Post Distortion for LED Communications with Orthogonal Polynomial Based Joint LED Nonlinearity and Channel Estimation," *IEEE Photonics Journal*, vol.10, no.4, pp.1-11, August, 2018.

3. Weikang Zhao, Qinghua Guo, Yanguang Yu, Jiangtao Xi and Jun Tong, "Iterative Nonlinearity Mitigation and Decoding for LED Communications," vol.30, no.19, pp.1731-1734, 1 Oct.1, 2018 *IEEE Photonics Technology Letters*.

List of Abbreviations

AWGN	Additive white Gaussian noise
APP	*a posteriori* probability
EVM	Error vector magnitude
FDE	Frequency domain equalization
IM/DD	Intensity modulated direct detection
ISI	Inter-symbol interference
LS	Least square
LEDs	Light-emitting diodes
LOS	Line of sight
LLRs	Log-likelihood ratios
ML	Maximum likelihood
NMSE	Normalized mean square error
OOK	On-off-keying
OFDM	Orthogonal frequency division multiplexing
PAPR	Peak-to-average power ratio
PAM	Pulse amplitude modulation
PPM	Pulse position modulation
RLS	Recursive least squares
SISO	Soft-in-soft-out
SER	Symbol error rate

Contents

List of Figures

List of Tables

Chapter 1

Introduction

1.1 Recent Development and Trends in LED Communications

In recent years, light-emitting diodes (LEDs) technology, known as "Green Illumination", is growing rapidly. Compared to traditional incandescent and fluorescent lights, LEDs have long life expectancy, high tolerance to humidity, low power consumption, small size and minimal heat generation [1]. Such huge advantages make LEDs capturing the market quickly and the world is in the critical period of upgrading Green Illumination LED lights. Table 1.1 shows the timetable for the elimination of incandescent lights and the promotion of LEDs around the world. Undoubtedly, LEDs is going to be the next generation lighting facility in the future. Another important feature of LEDs is that they are semiconductor devices capable of fast switching with the addition of appropriate drivers [2]. LEDs can flicker millions of times within 1 second and such high frequency cannot be noticed by human eyes but detected by photosensitive sensor.

Table 1.1: Timetable for the elimination of incandescent lights and promotion of LEDs.

China	Ban imports and sales of 15 watt and higher incandescent bulbs from 1 October 2016
USA	Replace incandescent light with LEDs between 2012 and 2014
Russia	Ban the production and sales of incandescent in 2012
European Union	Ban of all the use of incandescent lights in 2014
Australia	Stop the production of incandescent lights in 2009 and ban the use in 2020

Visible light emitted by LEDs can be modulated for simultaneous illumination and data transmission. LED communication technology is a promising field which offers a novel scheme of high-speed data transmission for indoor communications [3]. As a newly-developing wireless communication technology, it is getting more and more attention and has several advantages over traditional radio frequency (RF) communications.

- One of the most important merits is that it makes use of the existing LEDs to achieve simultaneous illumination and data transmission. As LED lights are ubiquitous in the world, any of the lights can be an access point. LED communications can be achieved based on the existing LED lighting facilities at low cost as there is no need for massive infrastructure construction [4].

- With the rapid development of information technology, the spectrum region of traditional RF resources is in high tension. Visible light has unregulated spectrum region and interferences with radio bands can be avoided [5].

- Visible light cannot pass through walls, so it is easy to achieve secure transmis-

sion within a certain room and prevent interferences from other places. It has the potential applications for military or information security fields.

- Traditional RF systems are prohibited or restricted in some occasions due to safety reasons, for example, in hospital, airplane, oil, gas well, etc., LED communications can avoid interference with existing electronic devices and prevent explosion and be an alternative option.

1.1.1 Applications of LED Communications

Besides simultaneous indoor illumination and data communication, there are many applications for LED communications. For example, indoor positioning system [6–8], LEDs on the celling can be used to determine the position of a person or any objects within a room. It is a good supplementary for the current global positioning system (GPS), which has difficulty to achieve accurate indoor positioning. LED communications is very popular for under water communications recently. Traditional under water communication relies on acoustic technology, however, due to the complicated under water environment it has many constraints and very low transmission speed [9]. Underwater optical wireless communication has the potential of achieving much better performance [10–12]. More and more vehicle manufactures are replacing the light by LEDs, so does the traffic lights and street lighting infrastructure [13]. LED communications make the interactions between cars to cars and cars to traffic or road lights possible, which can be exploited to build intelligent transportation systems or active safety systems [14, 15].

1.1.2 History and Development of LED Communications

Therefore, LED communication technology is an extremely promising field. Over the years, it has attracted a lot of research attentions all over the world and is developing rapidly. Research on indoor LED communications was firstly carried out in Japan. In 2000, Tanaka, etc. [16, 17] from KEIO University proposed the idea of LED-based wireless communications and did some feasibility analysis. They found that inter-symbol interference (ISI) and multipath propagation are two important factors that affect the overall system performance [18]. In 2003, Komine proposed the combination of power line communication and indoor LED communications [19]. In Europe 2008, OMEGA European project [20–22], also known as the Home Gigabit Access project was put forward aimed at combing LED communication technology, wireless and power line communications to achieve the future Internet. At the same time, USA also started a "Smart Lighting" Project, which lasts for 10 years and researchers from more than 30 universities are involved in. The project required to achieve communications between wireless terminals and LED lights. Not only that, IEEE established visible light communication group IEEE 802.15.7 in 2008. In 2011, Harald Haas, Professor from the University of Edinburgh firstly named visible light communications (VLC) as Light Fidelity (LiFi) [23]. And later he clarified that by making use of LEDs, LiFi takes VLC further to achieve fully networked wireless systems, which brought LED communications to a new chapter [24, 25].

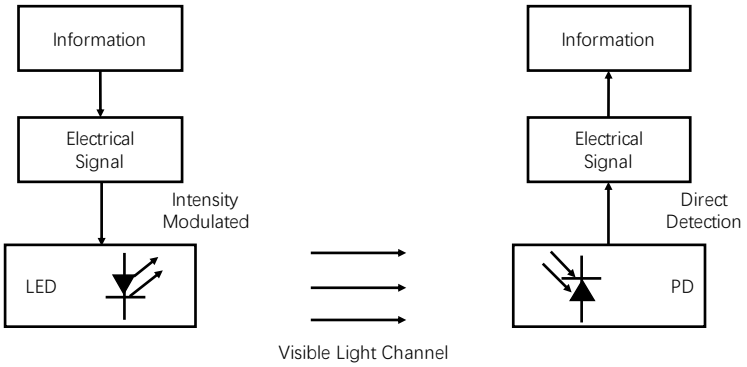

Figure 1.1: System description of LED communications.

1.1.3 System Description of LED Communications

Fig. 1.1 shows the system description of LED communications. In LED communication system, intensity modulated direct detection (IM/DD) system is being used [26]. At the transmitter side, information bits are firstly modulated to electric signals and are represented by voltage. This means that the electric signals can only take positive values, so modulation techniques commonly used in radio communications cannot be used without modifications. Then, it will be modulated to optical domain through the intensity of the LED light. After transmitted through the optical wireless channel, at the receiver side, the signal is detected by a photo diode (PD), which converts the optical intensity signal back to electric signal.

1.2 Research Motivations

Currently, there are two types of commercially white LEDs [27]. The first one has separate red-blue-green (RGB) emitters as a package and proper mixing of the RGB lights produces white light. The merits of this type of LEDs are, for example, it is easy to achieve colour rendering and it has wide bandwidth, which has the possibility of using wavelength division multiplexing (WDM) to significantly increase data rate [28]. How-

ever, RGB-LED is usually expensive in the market and it has different attenuations of RGB, which requires the receiver be able to detect multiple wavelengths when WDM is implemented [29]. The other type of LED consists of a single blue emitter and phosphor on top of it. The mix of blue and phosphor generates yellow light. It has limited modulation bandwidth due to the slow response of the phosphor [30, 31]. The single blue-chip LED is very popular and common in the market because it is cost efficient and stable [32].

To achieve data communications on either types of LED, various efficient modulation techniques that are suitable for IM/DD system are needed. The most widely used modulation technique is on-off-keying (OOK), also known as 2 amplitude-shift keying (2ASK), which merely relies on switching the light source on and off [33, 34]. In OOK modulation, the amplitude of the carrier wave only has two statuses and it corresponds to binary information 0 and 1, respectively. This binary modulation scheme is easy implementation and straightforward, however, it offers low spectral efficiency [26]. To enable higher data rates, more advanced modulation schemes are necessary. Orthogonal frequency division multiplexing (OFDM) technique is widely used in wired and wireless communication systems because of its inherent robustness to inter-symbol interference (ISI) since the symbol period is longer than the delay spread caused by multipath distortion [35]. Also, it has the advantage of using a simple one tap equalizer at the receiver to minimize the channel effect. More importantly, OFDM has better bandwidth efficiency than conventional modulation schemes such as OOK and pulse position modulation (PPM) [36]. The use of M-QAM OFDM is able to deliver very high data rates [37]. In current research, majority of the work focus on finding new types of OFDM techniques designed for IM/DD optical wireless communication (OWC) systems [38–40].

In IM/DD optical wireless systems, the intensity of the light cannot be negative or imaginary whilst conventional OFDM signals are bipolar and complex. Researchers have created several different forms of optical-OFDM designed for IM/DD OWC systems. For example, asymmetrically clipped optical OFDM (ACO-OFDM) [41], DC biased optical OFDM (DCO-OFDM) [42], as well as many other techniques based on the above two forms are developed [43, 44].

However, apart from the limited modulation bandwidth of the blue-chip LED, the inherent significant nonlinearity of LED also causes small modulation index [45]. In LED communications, signals in electric domain are modulated to optical domain using the light intensity of LEDs. At the receiver side, the intensity of the light is detected by a photo detector and converted to electric signals [46]. As power amplifier is the major source of nonlinearity in radio frequency communications, the inherent nonlinearity of LEDs also causes nonlinear distortions and is a challenge for VLC communications [47, 48]. According to [49–51], the nonlinear behaviour of the LEDs transfer function distorts the amplitude of the signal. Additionally, lower peak of the signals are forced to be the minimum LED turn on voltage while higher peak signals are clipped to avoid reaching the maximum permissible voltage. Thus, the system can only work in a very limited quasi-linear area as the dynamic range of the modulation is significantly reduced by its nonlinearity [45]. Fig. 1.2 shows the V-I characteristic of LED [45]. Point C stands for the bias point and I_c is the current at this point. Points A and B are the minimum and maximum current within the quasi-linear segment, respectively. The modulation index can be calculated as

$$m = \frac{\delta}{I_c}.$$

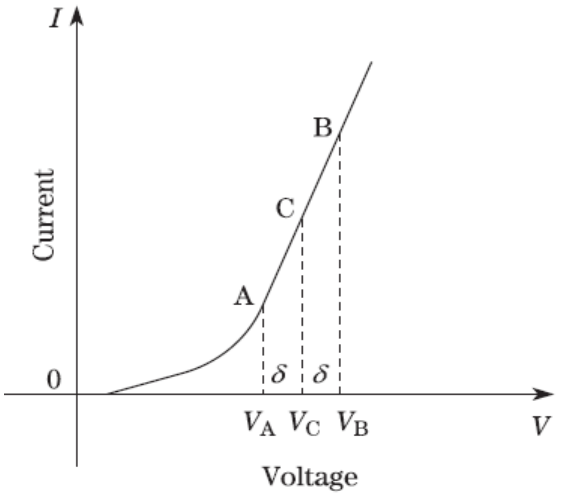

Figure 1.2: V-I characteristic of LED [45].

A big issue of using optical-OFDM in LED communications system is that OFDM suffers from large peak-to-average power ratio (PAPR) and high sensitivity to carrier frequency offsets [52]. For example, scaling and DC biasing could result in nonlinear signal distortions [53]. For an OFDM system to work successfully, the system needs a wide range of linearity to avoid distortion. Single-carrier (SC) modulation such as M-PAM and M-PPM does not have the limitations of OFDM. Also, it can be applied to IM/DD LED communication systems without signal clipping. SC modulation with frequency domain equalization (FDE) is a promising approach to ISI mitigation. It is shown in [35] that single carrier system delivers better performance than OFDM. It is worth highlighting that, single carrier system with frequency domain equalization has the same complexity with OFDM system in detection. SC-FDE overcomes all the limitation of OFDM and has its own advantage such as insensitive to carrier frequency and offset noise [54, 55]. It is worth and meaningful for us to study and develop a proper signal detection technology using SC-FDE in LED communication systems.

To avoid nonlinear distortions, some easy and straightforward approaches can be applied. For example, we can use binary modulation techniques such as OOK or pulse

position modulation (PPM), which are not affected by nonlinear effects [56]. A power back off technique (to keep input well within linear portion) is also a simple solution [57]. For optical-OFDM, there are some PAPR reduction techniques [58, 59] to decrease signal clipping at the expense of increasing system complexity. However, the above methods still suffer the small modulation index of LED and bandwidth efficiency is not increased. To fully make use of the input range of LEDs and increase modulation range, firstly, some nonlinear system identification techniques to model the nonlinear behaviour are needed. The overall nonlinear LED communication system can be expressed as follows [60]

$$y(n) = h(x(n)) + w(n), \tag{1.1}$$

where $y(n)$ is the received signals, $x(n)$ is the non-negative input signals to the LED and $w(n)$ is the additive noise. $h(\cdot)$ represents the nonlinear transfer function with the constraints that $I_{min} \leqq h(x(n)) \leqq I_{max}$. The characteristic of the nonlinear transfer function is determined by specific LEDs. For signals larger than the maximum permissible current I_{max} or lower than the minimum current I_{min}, double-sided clipping is applied. For signals within the LED input range, a nonlinear transfer function can be used to model the system nonlinear distortions. There are various nonlinear models that can be used to model the LED nonlinearity. Nonlinear models can be classified into memory and memoryless cases in terms of whether we consider the memory effects of LEDs. For the memory-less case, for example, a Taylor series or a polynomial are able to describe the nonlinear behaviour of a LED [61–64]. However, for high speed applications due to transport delay and rapid thermal effects, such nonlinear behaviour has memory effects and may vary with time, which cannot be ignored [60, 65, 66]. More complicated nonlin-

ear models with memory effects such as, Volterra series [67, 68], Winer model [69, 70], Hammerstein model [71] as well as memory polynomial [72] can be applied to model the LED nonlinearity and LED memory effect more accurately. Developing effective nonlinear system modelling method to identify the LED nonlinear behaviour is essential for the nonlinear distortion mitigation. In [57, 73–75], the authors proposed some adaptive least mean square (LMS) or recursive least squares (RMS) algorithms to estimate and update the parameters of the nonlinear model, but they are complicated and not easy in general. In [76], the author proposed to use orthogonal polynomials in replace of the conventional memory-less polynomial in order to solve the numerical stability when deriving the nonlinear model coefficients. However, the author only considered memory-less case and assumed Gaussian distribution. According to [76], developing closed-form expressions of the orthogonal polynomial basis for any other distribution is difficult in general. Considering the real-valued and non-negative constraints on the input distribution of LED communications, we believe developing special orthogonal polynomials for LED communications might be a solution for effective LED nonlinearity modelling.

With the knowledge of the system nonlinear functions, corresponding nonlinearity mitigation techniques are required to overcome the nonlinear distortions caused by LEDs. Currently, digital pre-distortion and post-distortion are two popular methods for solving the nonlinear distortions [77, 78]. Digital baseband pre-distortion [79–84] is the most popular technique for linearizing nonlinearity in high speed wireless applications. By identifying the characteristics of the nonlinear system, a pre-distorter, which has the inverse behaviour of the nonlinearity, is put in front of the nonlinear system to compensate the distortion. There are two major issues in digital baseband pre-distortion. Firstly, for direct learning approach [85], an effective system modelling method to identify the

nonlinear behaviour is required. Then, a proper method is required to accurately find the inverse of the nonlinear characteristics based on the system identification. However, according to [85], inversion of a nonlinear system cannot be easily achieved and sometimes even only possible within a limited range of input. Also, a nonlinear system of finite order of polynomial cannot be completely compensated by another finite order polynomial [86]. Errors are inevitably generated when deriving the inverse of the nonlinear model. Moreover, the inverse nonlinear operation to the received signal will cause colour noises. There is also an indirect learning approach that does not require the knowledge of nonlinear coefficients. A post-inverse filter of the nonlinear model is derived at the receiver side and then it is used as a pre-distorter at the transmitter side [85]. However, the method suffers from the noisy output of the nonlinear device [87]. In theory, pre-distortion has better performance over post-distortion as noise is not affected at the transmitter side. However, pre-distortion techniques are not cost-efficient as it needs feedback path from the receiver to transmitter. Additional physical modules and circuits are needed, which increases the system complexity and power efficiency. Post-distortion is receiver side nonlinearity mitigation technique, which has the advantage of no demand for additional physical circuits between transmitter and receiver. However, the biggest problem of current post-distortion techniques is that noise is added at the receiver side. Noise affected nonlinear distorted signals are forwarded to post-distortion, which is another nonlinear process. Gaussian distributed white noise will be converted to coloured noise, resulting signals in the most severe nonlinear interval suffers most, which will dominant the overall system performance. Also, modelling the post-distorter using finite order of the polynomial has residual nonlinear error as pre-distortion. As post-distortion is implemented at the receiver side, it is more convenient to use and adaptive post-distortion can

be easily realised to handle the time-varying nonlinearity of LEDs. We want to study and develop effective post-distortion technique for LED communications.

Another challenge in LED communications is that in indoor environment optical receivers may receive signals propagated from LEDs through multiple paths, for example, line of sight (LOS) propagation and non-LOS propagation which is also known as diffuse link due to reflections of room surfaces or other objects [88]. Such multipath propagation easily leads to severe ISI distortions, especially in high speed applications [18, 28]. Also, the memory effects in LED nonlinear distortions can be regarded as another type of ISI. Moreover, according to [89] and [90], the bandwidth limitation of LED induced fading will also lead ISI to the system. We want to study and develop effective signal detection technique to combat the above problems.

1.3 Research Contributions

The primary objectives of this thesis are to develop effective and efficient LED nonlinearity modelling and proper nonlinearity mitigation as well as real signal detection techniques to mitigate the nonlinear and ISI distortions in LED communications. To be more specific, the contributions of this thesis are as follows:

(1) In Chapter 3, we firstly review the conventional LED nonlinearity modelling methods using memory polynomials and show that the estimation of the memory polynomial coefficients suffers from numerical instability problem, resulting in inaccurate modelling and poor performance in nonlinearity mitigation. To solve the above problem, we propose an alternative LED nonlinearity modelling technique based on orthogonal polynomials. Considering the IM/DD modulated LED signals, we de-

velop a special set of orthogonal polynomial basis for PAM LED signals in order to achieve effective and efficient LED nonlinearity modelling. Due to the use of the orthogonal polynomials, the new basis matrix for the nonlinear model is a quasi-orthogonal matrix, avoiding the numerical instability problem during the estimation of the polynomial coefficients, which leads to low complexity and accurate LED nonlinearity modelling. Furthermore, we design a pre-distorter to mitigate the LED nonlinearity as well as the memory distortions.

(2) In indoor LED communications, multipath dispersion can lead to ISI at high data rates which cannot be ignored. We combine the ISI distortions due to multipath propagation, the limited bandwidth of LED and the memory effects as a whole composite ISI channel and then extend our previous work on orthogonal polynomial based LED modelling. We propose a joint LED nonlinearity and composite ISI channel estimation technique based on orthogonal polynomials for LED communications. Then, we applly low complexity frequency domain equalization to eliminate the ISI distortion due to the LED memory effects and optical ISI channel. A post-distorter is employed to mitigate the memory-less LED nonlinearity after FDE.

(3) With effective LED nonlinearity modelling technique described above, we consider a coded LED communication system and propose a very different iterative post-distortion technique based on maximum likelihood (ML) soft post-distorter and decoding. Rather than directly finding the non-distorted signals as the traditional post-distorters do, our ML-based soft post-distorter iteratively finds the *a posteriori* probability (APP) estimates of the data symbols based on the nonlinearity parameter and *a priori* information from the soft-in soft-out (SISO) decoder. Extrinsic information

in the form of log-likelihood ratios (LLRs) will be then passed through the SISO decoder. The advantage of our proposed method is that rather than finding the inverse of a nonlinear function using the finite order of a polynomial as a post-distorter, which will inevitably have residual modelling error, our method only requires the knowledge of the nonlinear coefficients. Also, our ML-based soft post-distorter is not a nonlinear process comparing to the traditional one, therefore, the distribution of the noise will not be affected. Simulations show that by taking advantage of the iterative processing between the SISO post-distorter and SISO decoder, our proposed method can achieve a significant system improvement than the traditional post-distortion technique. The performance achieved by our proposed technique is very close to that of the pre-distortion techniques, whilst holds much lower overall system complexity and computation cost.

1.4 Thesis Organization

The remaining thesis is organized as follows. In Chapter 2, we do a literature review of current research on LED communications. Firstly, we introduce the overall system structure and the IM/DD system for LED communications. Secondly, various modulation techniques specially designed for LED communications are described. Then, we introduce the LED nonlinearity problem and some popular nonlinear models being used for system modelling. Lastly, we review and compare some current works on nonlinear system modelling and some nonlinearity mitigation techniques. In Chapter 3, we focus on LED nonlinear system modelling and mitigation using memory polynomials. By solving the numerical instability in the conventional estimation technique, we develop

orthogonal polynomial basis for LED communication with PAM signalling for the first time and an effective LED nonlinearity modelling technique based on memory orthogonal polynomials is proposed. In Chapter 4, we consider both the LED nonlinearity with memory effect and ISI optical wireless channel. We develop a joint estimation approach to LED nonlinearity and composite ISI channel based on our orthogonal polynomial technique in Chapter 3. We design a receiver which consists of three modules including nonlinearity and composite channel estimator, FDE equalizer and nonlinearity mitigator. In Chapter 5, we develop a SISO post-distorter and combine it with a de-mapper in a coded LED communication system to handle the distortion of LED nonlinearity and ISI due to LED memory effect and optical wireless channel. Chapter 6 concludes the whole thesis work and address some future work for further study.

The notations used in this thesis are as follows. Lower case and upper case letters (e.g., x and X) denote scalars. Bold lower case letter (e.g., $\mathbf{x}$) denote column vectors and bold upper case letter (e.g., $\mathbf{X}$) denote matrices. The superscripts "H" denotes the conjugate transpose operation and symbol $\mathbf{I}$ represents an identity matrix with proper size.

Chapter 2

Literature Review of LED Communications

This chapter provides an overall literature review of LED communications system. Firstly, we introduce the whole system structure and review various modulation techniques designed for LED communications. Secondly, we focus on the LED nonlinear problem and describe the impact of nonlinear distortions, which needs to be carefully handled to avoid severe system degradation. Then, we introduce and compare many of the commonly used nonlinear models (e.g., Volterra series, memory polynomials) for effective nonlinear system modelling. Lastly, we do a thorough review and comparison of the current work on nonlinear system modelling and nonlinear mitigation techniques, including the most popular pre-distortion and post-distortion techniques.

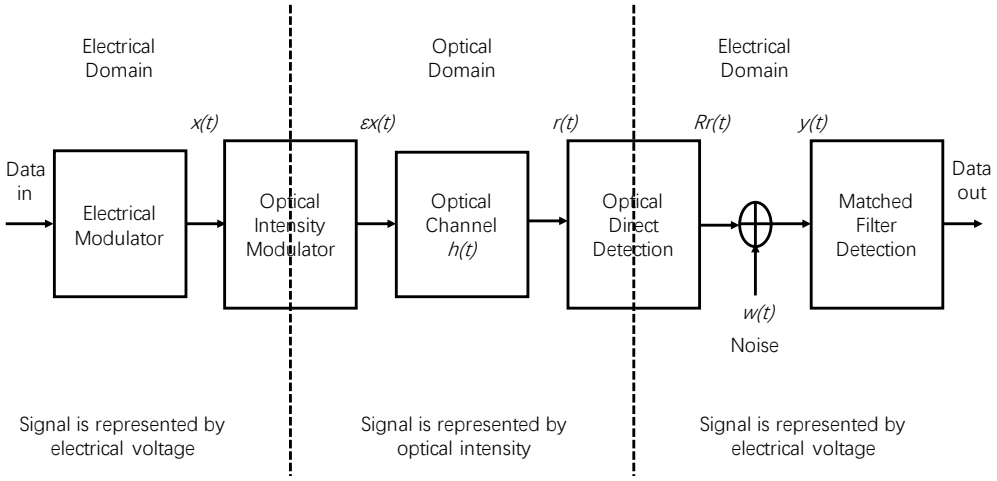

Figure 2.1: Intensity modulated direct detection system [91].

2.1 Intensity Modulated Direct Detection System

Fig. 2.1 shows the block diagram of the intensity modulated direct detection (IM/DD) system being used in LED communications [91]. At the transmitter side, firstly information data is modulated in electrical domain and is represented by electrical voltage $x(t)$. Then, it is scaled by an optical intensity modulator and represented by the optical intensity of LED. Transmitted signals $x(t)$ must be real and non-negative as they are being modulated onto the intensity of the light using LED, which means that modulation techniques commonly used in traditional radio frequency (RF) communications must be modified to use in IM/DD systems [92]. After transmitting through the optical wireless channel with impulse response $h(t)$, at the receiver side, signal is directly detected by a photo diode, which converts the optical signal back to electrical signal. The received signal can be represented as

$$y(t) = R\epsilon x(t) \otimes h(t) + n(t), \tag{2.1}$$

where symbol $\otimes$ denotes convolution, R is the responsivity of the photo diode and $n(t)$ is modelled as additive white Gaussian noise (AWGN) added in the electric domain. Different from the conventional RF communication systems, in LED communications, the transmitted signal $\epsilon x(t)$ is the instantaneous optical power of the LED and the average transmitted optical power P_t is calculated as

$$P_t = \lim_{T\to\infty}(\frac{1}{2T})\int_{-T}^{T}\epsilon x(t)dt, \tag{2.2}$$

which is proportional to the input power signal $x(t)$ rather than the usual square of the signal amplitude $x^2(t)$.

2.2 LED Communications Modulation Technology

In IM/DD LED communications systems, since the transmitted signal must be real and non-negative, several single carrier modulation techniques can be exploited straightforwardly, for example, on-off keying (OOK), unipolar pulse-amplitude modulation (PAM) and pulse-position modulation (PPM). Popular multi-carrier modulation schemes such as OFDM has also been modified to meet the requirements for optical wireless communications and it is named as optical-OFDM.

There are many different modulation schemes appropriate for optical wireless communication systems which has its own merits and demerits. As LEDs has limited modulation bandwidth and the problem of nonlinear distortions, modulation techniques which are sensitive to these factors should be considered. For indoor visible light communications, average transmitted optical power is constrained due to eye safety requirement [93]. In order to keep the average transmission power down, modulation techniques

with high power efficiency is needed. Also, considering the multipath optical wireless channels and LED memory effects, ISI distortion is another problem in LED communications. Criterions for evaluating efficient and effective optical IM/DD modulation techniques include power efficiency, bandwidth efficiency as well as robustness or solutions to ISI. This section introduces and compares the various modulation techniques being used in LED communications.

2.2.1 OOK modulation

Among all the modulation techniques that are appropriate for IM/DD optical wireless communications, the binary modulation scheme OOK which merely relies on switching the light source on and off is one of the most popular and easy implementation one. Within a symbol period, the LED light on represents bit "1" while the light off stands for bit "0". OOK is easy and straightforward and can be applied to LED communications directly. Majority research of the feasibility analysis and preliminary experiments of LED communications use OOK modulation as it offers a good compromise between complexity and system performance. Reducing the duty cycle of OOK modulation increases the bandwidth, however, OOK is not efficient especially at small duty cycles [94]. Considering the limited modulation bandwidth of LEDs, more efficient higher order modulation techniques are required to achieve better system performance.

2.2.2 Optical-OFDM

Orthogonal frequency division multiplexing (OFDM) technique is being widely used in conventional wired and wireless radio frequency communications due to its inherent robustness to ISI caused by multipath channel [39]. Also, it is simple implementation

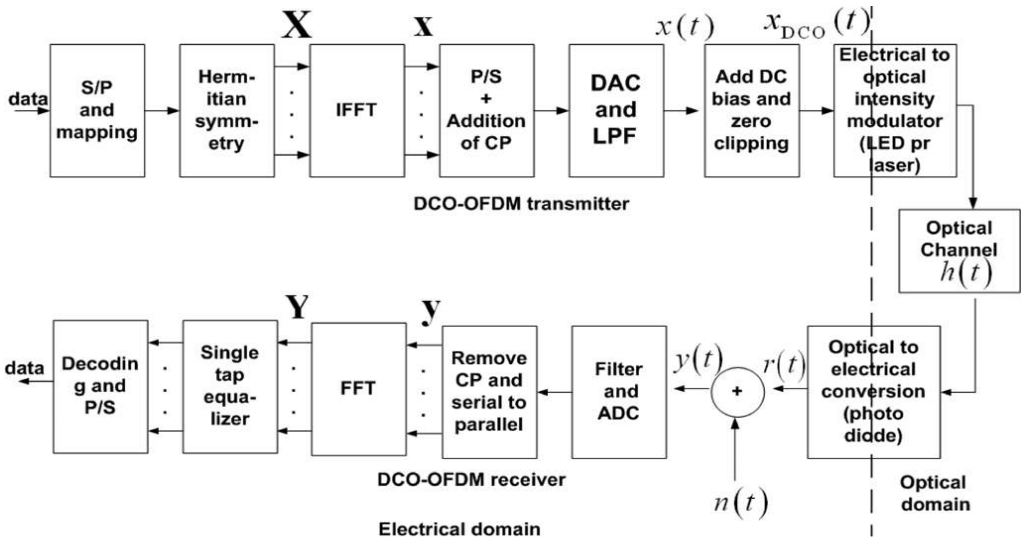

Figure 2.2: Block diagram of DCO-OFDM [36].

and has the advantage of using a simple one tap equalizer at the receiver to minimize the channel effect. More importantly, OFDM has better bandwidth efficiency than conventional modulation schemes such as OOK and pulse position modulation (PPM) [95]. The use of M-QAM OFDM has the potential for delivering very high data rates [96]. In the past years, majority of the work has been done focus on finding new types of OFDM techniques designed for IM/DD optical wireless communication systems. In order to make the transmitted bipolar and complex OFDM signals real and non-negative, several different types of optical-OFDM techniques for IM/DD system has been proposed, for example, DC biased optical OFDM (DCO-OFDM) [97], asymmetrically clipped optical OFDM (ACO-OFDM) [41] and many other developed techniques based on the above two forms.

DCO-OFDM

Fig. 2.2 shows the block diagram of a DCO-OFDM system. The bipolar and complex data signal $\mathbf{X} = [X_0, X_1, X_2, ..., X_{N-1}]$ is the input to the inverse fast Fourier transform (IFFT) operation. The input $\mathbf{X}$ is required to have Hermitian symmetry property defined

as follow,

$$X_m = X^*_{N-M} \quad 0 < m < N/2, \tag{2.3}$$

where the two elements $X_0 = X_{N/2} = 0$. The Hermitian symmetry property of the input ensures the output of the IFFT signal **x** to be real but not complex. The *nth* time domain of **x** is expressed as

$$x(n) = \frac{1}{N}\sum_{m=0}^{N-1} X_m exp(\frac{j2\pi nm}{N}), \tag{2.4}$$

where N is the number of points of the IFFT operations and X_m is the *mth* subcarrier of the input signals. In DCO-OFDM, all subcarriers carry data symbols, however, due to the Hermitian symmetry property only $(N/2 - 1)$ subcarriers carry unique data. After digital to analog (D/A) conversion and low pass filtering, an appropriate DC bias is added to $x(t)$ and any remaining negative signals are clipped generating the DCO-OFDM signals $x_{DCO}(t)$. All the subcarriers will be affected by the clipping noise as they all carry information. $x_{DCO}(t)$ will be the input to the optical intensity modulator and at the receiver side, the OFDM receiver is similar to the conventional one. DCO-OFDM is less efficient in terms of the average optical power due to the DC bias added at the transmitter side.

ACO-OFDM

Fig. 2.3 shows the block diagram of a ACO-OFDM system. Only odd components of the complex input signal **X** carry information, so that the input to the IFFT operation $\mathbf{X} = [0, X_1, 0, X_3, ..., X_{N-1}]$. Also, the input signals are required to have Hermitian symmetry property as the DCO-OFDM one. After IFFT operation, the time domain signal **x** is real

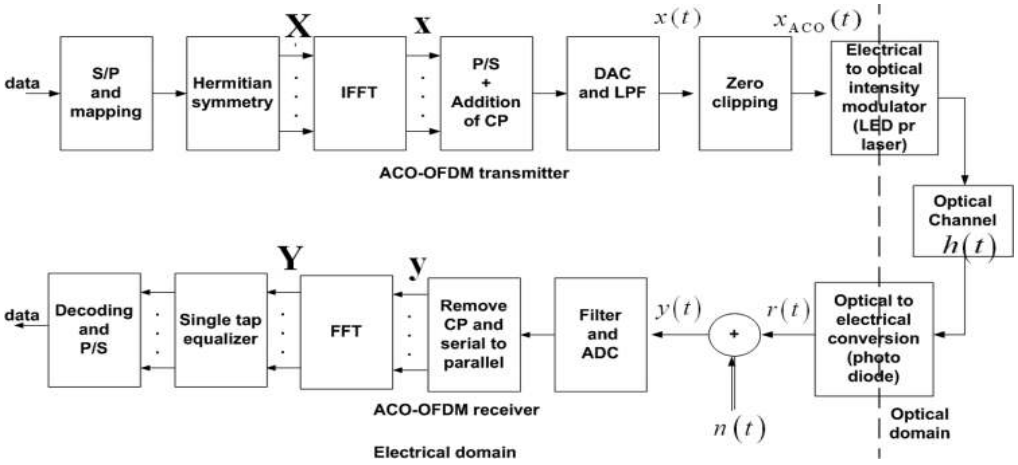

Figure 2.3: Block diagram of ACO-OFDM [36].

and has the following anti-symmetry property [43],

$$x(n) = -x(n + \frac{N}{2}) \quad 0 < k < \frac{N}{2}. \tag{2.5}$$

Before modulating onto the intensity of the light, $x(t)$ is clipped at zero to ensure all the resulting ACO-OFDM signals $x_{ACO}(t)$ are non-negative. Due to the anti-symmetry property of the input signal, the clipping operation will not lead to any loss of information as the clipping noise falls on even subcarriers [41]. In ACO-OFDM, as only odd subcarriers transmit data symbols and due to the anti-symmetry, merely $(N/4)$ subcarriers carry unique data, which is half of the DCO-OFDM. The receiver is similar to the DCO-OFDM while only odd subcarriers need to be modulated. ACO-OFDM is less efficient in terms of bandwidth as only half subcarriers carry data.

ADO-OFDM

Asymmetrically clipped DC biased optical OFDM (ADO-OFDM) that combines the advantages of ACO-OFDM and DCO-OFDM is then developed. In the ADO-OFDM system, ACO-OFDM is used on the odd subcarriers while DCO-OFDM is used on the even

subcarriers. Because all the subcarriers are used to carry data, the bandwidth efficiency is better than ACO-OFDM. Also, due to the use of the more power efficient ACO-OFDM on half of the subcarriers, the overall optical power efficiency is better than DCO-OFDM [36].

Drawbacks of Optical-OFDM

Optical-OFDM has many advantages, however, it also has many drawbacks in LED communications due to the inherent nonlinearity of LEDs. Among all these, two of the most crucial issues are the high peak-to-average power ratio (PAPR) of the OFDM signals and the in-band distortion caused by the LED nonlinearity.

PAPR is defined as the ration between the maximum transmitted instantaneous power and the average transmitted power

$$PAPR = \frac{max(|x(t)|)^2}{E(|x(t)|)^2}, \tag{2.6}$$

where $E[\cdot]$ represents expectation operation. Because of the existence of a huge number of independently modulated subcarriers in the OFDM signals, the PAPR could be very high. An OFDM system needs wide range of linearity to avoid distortion, for example, the input of the IFFT transmitter and output of the FFT receiver are required to be approximately linear to achieve better system performance [98]. However, in LED communications, LED is the major source of nonlinearity, in order to ensure the input signals stay in the working region, clipping and DC biasing could result in signal distortions. Also, the nonlinear conversion of the OFDM signals will cause nonlinear distortions during the equalization process which significantly affects the overall system

performance.

Due to the nonlinearity of the LED, optical-OFDM signals will also cause in-band distortion and inter-carrier interference (ICI) which is another serious problem [99, 100]. We consider the complex baseband ACO-OFDM signal as

$$x(n) = \frac{1}{N}\sum_{m=0}^{N-1} X_m exp(\frac{j2\pi nm}{N}), \quad n = 0, 1, 2, ..., N-1 \tag{2.7}$$

where N is the number of points of the IFFT operations, X_m is the *mth* subcarrier of the input complex signals and n is the discrete time domain index. After clipping, ACO-OFDM signal $x_{ACO}(n)$ is the input to the optical intensity modulator. To simplify the calculations, we choose the LED nonlinearity as a simple 3rd order memoryless polynomial and consider only the odd order nonlinearity according to [99], it can be expressed as

$$y(n) = a_1 x_{ACO}(n) + a_3 x_{ACO}(n)^3, \tag{2.8}$$

where $y(n)$ is the received signal and a_1, a_3 are the nonlinear coefficients. Assuming AWGN channel, the signal after FFT operation can be calculated as

$$\widehat{X}_m = \sum_{m=0}^{N-1} y(n) exp(-\frac{j2\pi nm}{N}) + w(m), \quad m = 1, 3, 5, ... \tag{2.9}$$

where $\widehat{X}_m$ is the *mth* subcarrier of the received symbol and $w(m)$ represents AWGN and clipping noise. Substitute (2.8) into (2.9), we have

$$\begin{aligned}\widehat{X}_m &= \sum_{m=0}^{N-1} a_1 x_{ACO}(n) exp(-\frac{j2\pi nm}{N}) + \sum_{m=0}^{N-1} a_3 x_{ACO}(n)^3 exp(-\frac{j2\pi nm}{N}) + w(m) \\ &= \alpha + \beta + w(m) \quad m = 1, 3, 5...\end{aligned} \tag{2.10}$$

where

$$\begin{aligned}\alpha &= \sum_{m=0}^{N-1} a_1 x_{ACO}(n) exp(-\frac{j2\pi nm}{N}) \\ &= a_1 X_m \quad m = 1, 3, 5, ...\end{aligned} \tag{2.11}$$

And β represents the nonlinear distortion which can be further solved as

$$\begin{aligned}\beta &= \sum_{m=0}^{N-1} a_3 x_{ACO}(n)^3 exp(-\frac{j2\pi nm}{N}) \\ &= a_3(x_{ACO}(0)x_{ACO}(0)^2 + x_{ACO}(1)x_{ACO}(1)^2 exp(-\frac{j2\pi m}{N}) + ... \\ &+ x_{ACO}(N-1)x_{ACO}(N-1)^2 exp(-\frac{j2\pi(N-1)m}{N})) \quad m = 1, 3, 5, ...\end{aligned} \tag{2.12}$$

Let $x_{ACO}(n)^2 = \omega_n$ and substitute $x_{ACO}(n)$ with equation (2.7), we have

$$\beta = \frac{a_3}{N}(\sum_{m=0}^{N-1} \omega_n exp(-\frac{j2\pi nm}{N}) \sum_{p=0}^{N-1} X_p exp(\frac{j2\pi nm}{N})), \tag{2.13}$$

which are ICI added to the system. Rearranging equation (2.10),

$$\begin{aligned}\widehat{X}_m &= X_m(a_1 + \frac{a_3}{N}\sum_{m=0}^{N-1}\omega_n) + \frac{a_3}{N}\sum_{p=0,p\neq m}^{N-1} X_p(\sum_{m=0}^{N-1}\omega_n exp(\frac{j2\pi(-m+p)n}{N})) + w(m) \\ &= X_m \times \mu + \Omega + w(m),\end{aligned} \tag{2.14}$$

where

$$\mu = (a_1 + \frac{a_3}{N}\sum_{m=0}^{N-1}\omega_n) \tag{2.15}$$

represents the frequency shift and

$$\Omega = \frac{a_3}{N}\sum_{p=0,p\neq m}^{N-1} X_p(\sum_{m=0}^{N-1}\omega_n exp(\frac{j2\pi(-m+p)n}{N})) \tag{2.16}$$

is the nonlinear distortion noise.

2.2.3 PAM, PPM Modulation

Single carrier multilevel modulation techniques such as pulse-position modulation (PPM) and unipolar pulse-amplitude modulation (PAM) are also very popular to IM/DD optical wireless systems as they can be applied directly without any signal clipping.

In L-level PPM, there are L symbols for each symbol duration T, which is divided into L sub-intervals. The optical transmitter is on during one of these intervals and off for the rest of the time. PPM is a power efficient modulation technique and the higher the order of L, the better the power efficiency [93].

Unipolar PAM is a very straightforward and easy implementation technique. In L-level PAM, one of the L discrete amplitudes are used for transmitting data during each symbol interval. Compared to DCO-OFDM and ACO-OFDM that can only utilize $1/2$ and $1/4$ of the bandwidth, respectively due to Hermitian symmetry restriction, high level PAM is a more bandwidth efficient modulation technique. More importantly, PAM has low power consumption and low PAPR, which is a huge advantage over optical-OFDM in LED communications. Moreover, according to [35], given the same data rate, L-PAM with minimum mean-square error decision-feedback equalization (MMSE-DFE) achieves better system performance than all the optical-OFDM schemes with the advantage of high bandwidth efficiency. Single carrier frequency domain equalization (SC-FDE) has been proven as an attractive alternative to OFDM for RF communications, which has low PAPR, high tolerance to nonlinearity and overall similar complexity to OFDM. PAM with SC-FDE is getting increasing attention in LED communications and be a good alternative to optical-OFDM.

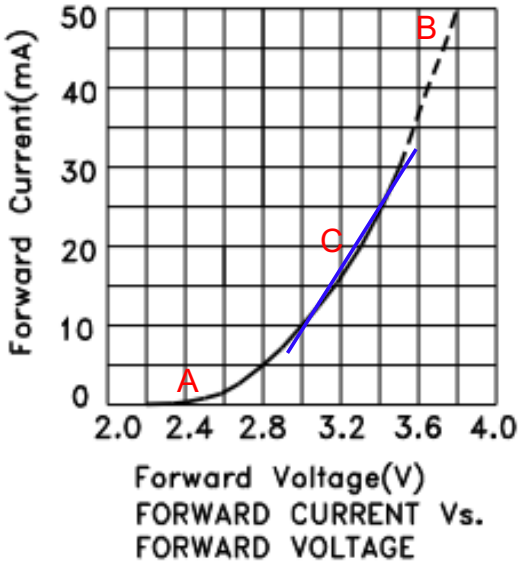

Figure 2.4: LED V-I curve datasheet [102].

2.2.4 CAP Modulation

As there are number of drawbacks in O-OFDM schemes, some other modulation schemes have recently been investigated such as PAM and carrier-less amplitude and phase (CAP) modulation. The bandpass CAP modulation is basically a QAM modulation where instead of using a mixer for up- and down-conversion, it employs two orthogonal finite impulse response (FIR) digital filters. So, the electrical signal that modulates the LED intensity is a DC-biased QAM signal on a sub-carrier of relatively low frequency. CAP modulation was considered for LED communications due to its advantages of low PAPR, high spectral efficiency and simple system structure [101].

2.3 LED Nonlinear Problem

Like Nonlinear distortions due to power amplifier in RF communications, nonlinear components in LED communications also lead to signal distortions and system performance degradation. LED is assumed to be the major source of nonlinearity in an optical

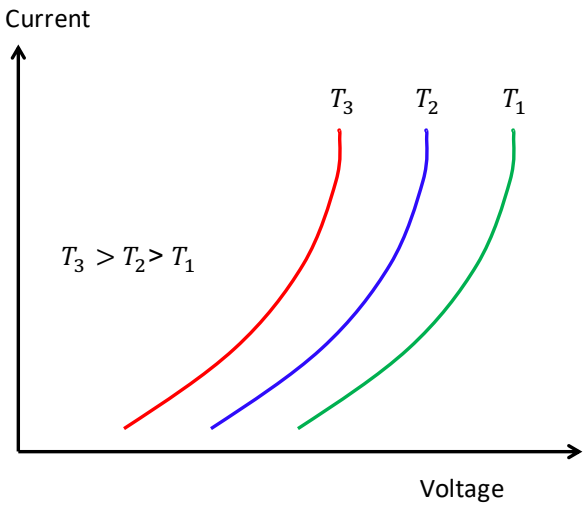

Figure 2.5: LED V-I curve with dynamic temperature change [60].

wireless communications system. Fig. 2.4 shows a typical datasheet of Kingbright Blue LED V-I curve [102]. The input signals must be larger than the LED turn-on voltage (point A), lower signals are clipped while signals higher than the maximum permissible voltage or the saturation point (point B) are also clipped to avoid overloading. The modulation range is limited to a quasi-linear segment (dashed line) to avoid nonlinear distortions. For signals beyond the quasi-linear region, the electrical to optical conversion is nonlinear. Both the nonlinear mapping within the LED working dynamic range and the clipping of signals below minimum turn-on voltage and maximum allowable voltage could result in nonlinear distortions. Moreover, due to transport delay, rapid thermal effects as well as biasing circuits that are dependent on signal envelope, such nonlinear behaviour has memory effects and varies based on the different present and previous input signals [65]. In addition, as shown in Fig. 2.5 the LED V-I characteristic may change over time due to the change of temperature and the age of the device [60, 61].

2.4 Nonlinear Models

Nonlinearity modelling is essential for system identification and the mitigation of nonlinear distortions in LED communications. The following part describes and compares some of the different nonlinear models being widely used.

2.4.1 Memoryless Polynomial

Nonlinear models can be classified into memoryless and memory cases. In terms of the memoryless model, in LED communications, only the amplitudes of the input signals are nonlinear functions of the transmitted instantaneous optical power. A memoryless polynomial can be used to model a LED nonlinearity without memory effects, it can be expressed by Taylor series as [60]

$$y(n) = \sum_{k=1}^{K} a_k x(n)^k, \tag{2.17}$$

where $x(n)$ is the electrical input signal and $y(n)$ is the output of LED. K is the order of the polynomial and a_k represents the nonlinear coefficients. The memoryless polynomial model is popular due to its simplicity and the coefficients can be determined based on the measured input and output relationship. However, for high speed communications, LED memory effects could not be ignored and more advanced nonlinearity models are required.

2.4.2 Volterra Series

Volterra series is a general nonlinear model with memory effects [67], which has been used to model with a wide range of nonlinear problems [68]. Fig. 2.6 shows the block

diagram of the general Volterra model. In discrete time, it can be written as

$$y(n) = \sum_{k=1}^{K} y_k(n), \tag{2.18}$$

$$y_k(n) = \sum_{m_1=0}^{M-1} \cdots \sum_{m_k=0}^{M-1} h_k(m_1, \cdots, m_k) \prod_{l=1}^{k} x(n - m_l), \tag{2.19}$$

where $x(n)$ is the input signal to the nonlinear system, and the output of the system is $y(n)$. K is the order of the Volterra nonlinear system and $y_k(n)$ is the k-dimensional convolution of the input with Volterra kernel h_k while M represents the length of the memory effects.

Volterra series can be used to properly model the LED nonlinearity including memory effects, however, it consists of a sum of multidimensional convolutions leading to high system complexity. A serious disadvantage is that a great number of parameters need to be estimated to model the system [103]. Finding the exact inverse of the system is difficult in general and it also requires the estimation of a large number of coefficients. To overcome the complexity limitation of the general Volterra model in practical systems, many other special simplified nonlinear models based on the Volterra series are developed, which makes the system implementation and parameter estimation easier. The various models are described in the following.

2.4.3 Winner Model

Winner model is a special case of the general Volterra series. It consists of a linear-time invariant (LTI) system that describes the LED memory effects and is followed by a memoryless nonlinearity. The block diagram of Winner model is shown in Fig. 2.7. It

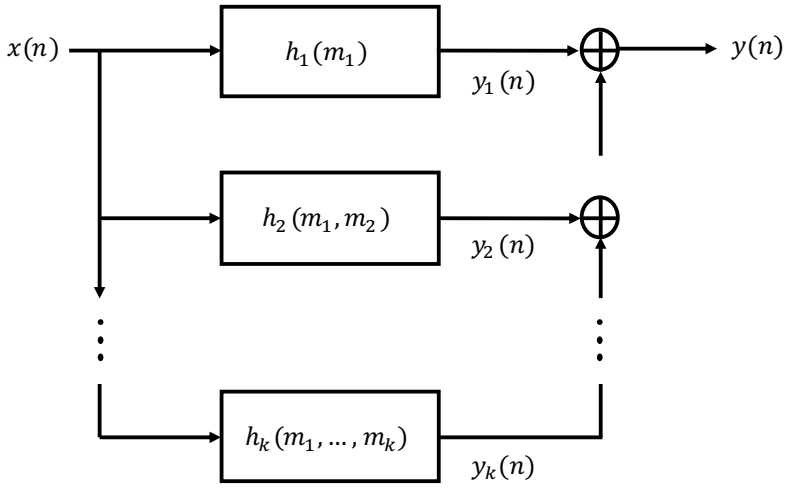

Figure 2.6: Block diagram of the general Volterra model.

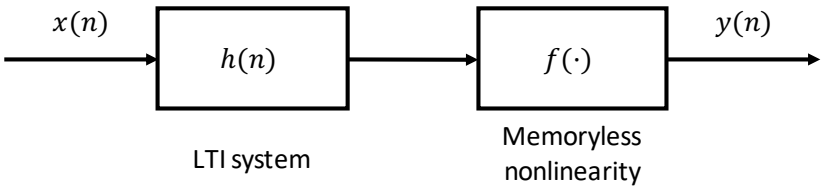

Figure 2.7: Block diagram of Winner model.

can be written as

$$y(n) = \sum_{k=1}^{K} a_k [\sum_{m=0}^{M-1} h(m)x(n-m)]^k, \tag{2.20}$$

where a_k is the coefficient of the memoryless nonlinearity and M represents the length of the memory. Winner model describes the nonlinearity with memory effects with much less complexity, however, one difficult is that the relationship between the output $y(n)$ and the coefficients $h(m)$ is nonlinear, which makes the extraction of $h(m)$ harder than the linear case [57].

2.4.4 Hammerstein Model

Hammerstein model is just the opposite of Winner model, which contains a memoryless nonlinearity followed by a LTI system. The block diagram of Hammerstein model is

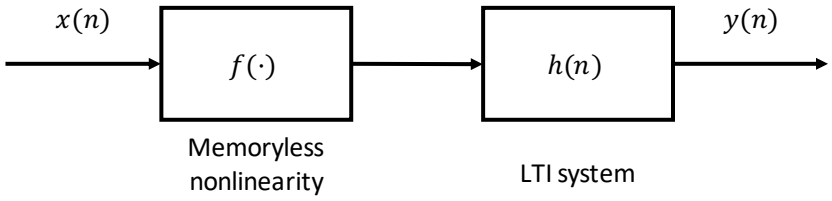

Figure 2.8: Block diagram of Hammerstein model.

shown in Fig. 2.8. It can be expressed as

$$y(n) = \sum_{m=1}^{M-1} h(m) \sum_{k=1}^{K} a_k x(n-m)^k. \tag{2.21}$$

This is also a simple nonlinear model with memory effects which is appropriate for general systems. The advantage of Hammerstein model is that the relationship between the memoryless nonlinear coefficient a_k and the LTI parameter $h(m)$ is linear, which makes the estimation easier.

2.4.5 Memory Polynomial

Another similar but simpler model than Volterra series proposed by Kim [72] and Ding [103] is the memory polynomials. It can be expressed as

$$y(n) = \sum_{k=0}^{K-1} \sum_{m=0}^{M-1} a_{km} x(n-m)|x(n-m)|^k, \tag{2.22}$$

where K is the order of the polynomial and M is the maximum memory depth. And a_{km} are two-dimensional coefficients that represents both the nonlinear and memory effects.

Memory polynomials is one of the very popular and common functions for nonlinear system and pre-distorter modelling in recent years [82]. It has been proven effective for pre-distortion and can offer a good compromise between generality and ease of pa-

rameter estimation and implementation.

2.5 Current Work on Nonlinearity System Modelling and Nonlinearity Mitigation

2.5.1 Straightforward Nonlinearity Mitigation Techniques

Once we have studied the impact of LED nonlinear distortions and different methods for nonlinear system modelling, it is essential to design some distortion mitigation techniques to overcome the nonlinear problem.

One simple solution is to use two-level modulation schemes such as OOK and PPM. Only two-level signals "0s" and "1s" are transmitted by turning the light on and off, which are immune to system nonlinearity. Another similar solution is to power back off the average transmitted signals [104]. In this way, most of the transmitted signals are kept well within the linear portion to avoid the nonlinear distortion. However, these above methods not only suffer power efficiency penalty but also have a very limited dynamic range for modulation resulting in low bandwidth utilization efficiency. The overall system performance is not improved.

Same as the power back off method, if optical-OFDM is used for modulation, some PAPR reduction techniques can be used to avoid the clipping of high level signals [105]. However, by using PAPR reduction technique, system complexity will be increased and bandwidth efficiency will be sacrificed. This method does not offer system improvement either.

All the above methods focus on how to avoid the nonlinear distortion rather than

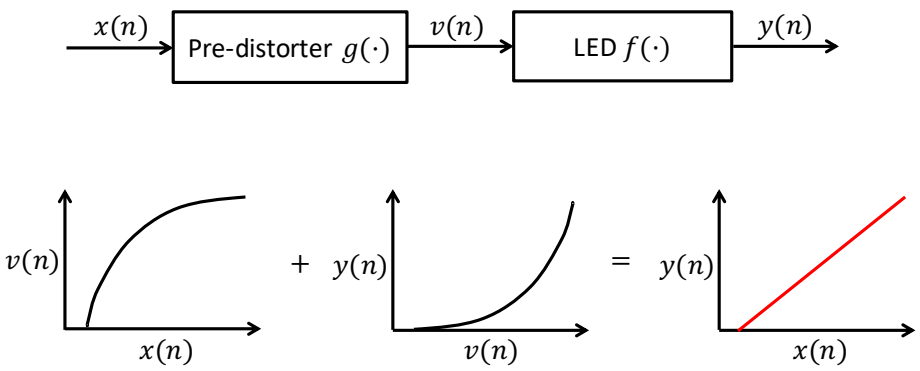

Figure 2.9: Block diagram of digital baseband pre-distortion.

linearizing the nonlinearity. With accurate nonlinear system modelling, nonlinearity mitigation technique is the most effective one to compensate the distortions and improve system performance. Among those, digital baseband pre-distortion and post-distortion are the most popular and effective nonlinearity mitigation techniques.

2.5.2 Digital Baseband Pre-distortion

Digital baseband pre-distortion is cost effective and suitable for linearizing nonlinearity in high speed wireless applications. By identifying the characteristics of the nonlinear system, a pre-distorter, which has the inverse characteristic of the nonlinearity, is put in front of the nonlinear system to compensate the distortion. As shown in Fig. 2.9, the input signal $x(n)$ is firstly passed through a pre-distorter, which generates pre-distorted signal $v(n)$. $v(n)$ is then modulated by a nonlinear LED and represented by the intensity of the light $y(n)$. The lower part of the figure shows the input and output relationship between $x(n)$, $v(n)$ and $v(n)$, $y(n)$. If the characteristic of the pre-distorter and LED are inverse, the input and output relationship of the system will be linear. For example, if

$$g(x(n)) \cdot f(v(n)) = G, \tag{2.23}$$

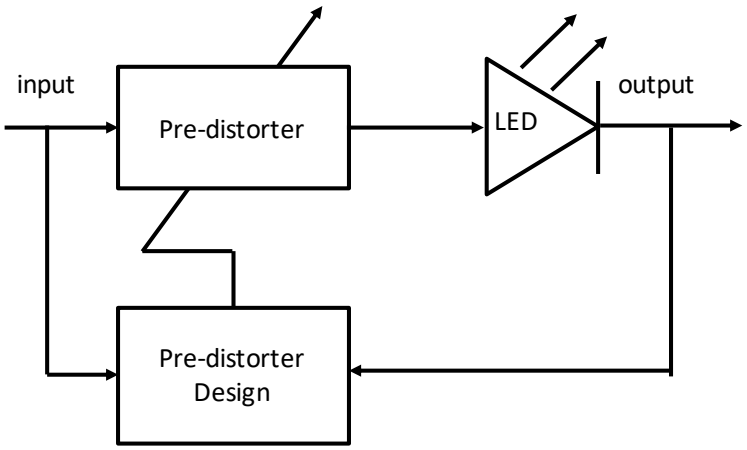

Figure 2.10: Block diagram of adaptive pre-distortion technique [60]

where G is the gain of the system. The input and output relationship of the system will be linear and can be represented as

$$y(n) = Gx(n). \tag{2.24}$$

As the characteristic of the LED may be changed due to temperature variation or ageing, sometimes adaptive pre-distortion techniques are required. As shown in Fig. 2.10, additional feedback path from the LED is needed, which increases computational complexity and power efficiency. However, this method can provide better performance as noise is not affected.

Direct learning

Pre-distortion technique can be divided into direct learning and indirect learning approaches. Direct learning requires the estimation of the nonlinear parameter in advance and the pre-distorter is calculated directly by finding the inverse of the nonlinearity. As shown in Fig. 2.11, it finds the pre-distorter adaptively by minimizing the difference between the LED input $x(n)$ and output $y(n)$ directly. This method can achieve

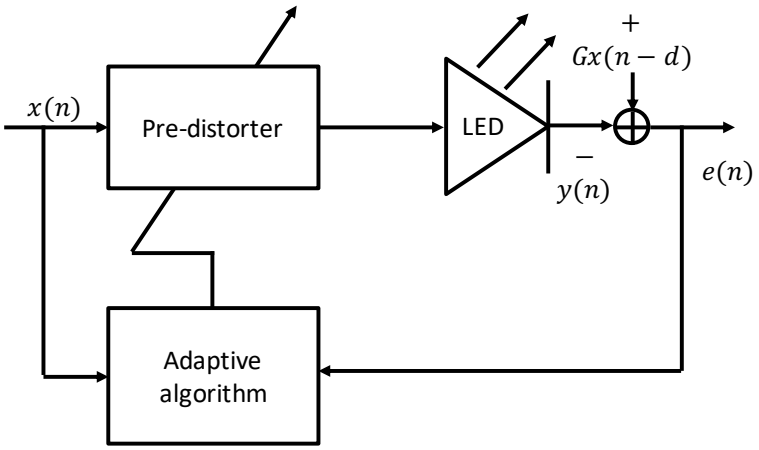

Figure 2.11: Block diagram of direct learning [106].

better performance as the coefficients of the pre-distorter is updated directly based on pre-distorter input and LED output. However, LED nonlinearity parameter must be estimated firstly and adaptive algorithm must be applied, which increase system complexity and computation cost.

Indirect learning

Indirect learning pre-distortion approach does not require the knowledge of the nonlinear model. As shown in Fig. 2.12, a virtual post-distorter of the nonlinear model is firstly derived, then copied and put in front of the LED as a pre-distorter. By minimizing the difference between the actual pre-distorter output $v(n)$ and the virtual post-distorter output $\hat{v}(n)$, the pre-distorter is updated and the post-distorter is removed when converges. The indirect learning approach is popular and cost efficient due to its less complexity as nonlinear model does not need to be identified. However, it needs a virtual post-distorter to model the inverse of the nonlinear model, a copy of the post-distorter in front of the nonlinear system affects performance. Also, the measurement of LED output $y(n)$ will be noisy [106].

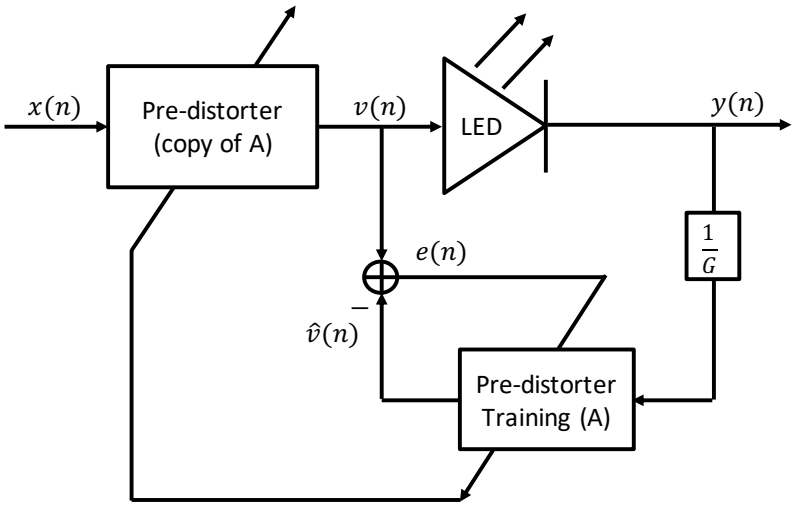

Figure 2.12: Block diagram of indirect learning [103].

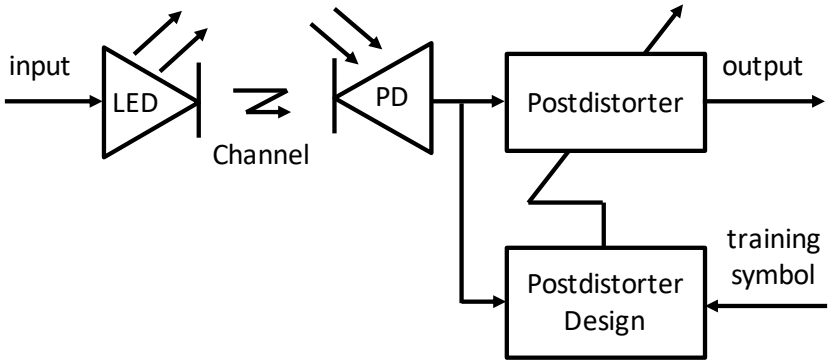

Figure 2.13: Block diagram of adaptive post-distortion.

2.5.3 Digital Baseband Post-distortion

Digital baseband post-distortion is a receiver side nonlinearity mitigation technique. As shown in Fig. 2.13, comparing to pre-distortion technique, adaptive post-distortion has the advantage of no demand for additional physical circuits between transmitter and receiver. Post-distortion is a straightforward, easy implementation, and more cost efficient nonlinearity mitigation technique, which is practical to achieve in real systems. However, as noise is added at the receiver side, noise affected nonlinear distorted signals are forwarded to post-distortion, which is another nonlinear process. The distribution of the noise will be changed from Gaussian distributed to coloured noise. In general, the

performance of post-distortion is worse than pre-distortion.

Chapter 3

Orthogonal Polynomial Based Nonlinearity Modelling and Mitigation for LED Communications

3.1 Introduction

LED is the major source of nonlinearity in LED communications, and the nonlinearity needs to be modelled effectively and thereby mitigated through pre-distortion or post-distortion to avoid degradation of communication performance. Thus, nonlinear system modelling and mitigation methods are essential for solving the distortions. In [107], LED nonlinearity is modelled using memoryless polynomials and then a pre-distorter which has the inverse characteristic of the polynomial model is designed to compensate for the nonlinearity. As LED nonlinearity may change over time due to temperature shift and component ageing, the mitigation techniques need to deal with the dynamic nonlinearity of LED. In [108], with a memoryless second order polynomial model, an

adaptive least mean square algorithm is designed for dynamic nonlinearity compensation. Because LEDs often exhibit nonlinearity with memory effects, especially for high speed transmission, memory-less polynomial are inadequate to model the LED nonlinearity. In [109], memory polynomial is used and a post-distorter is constructed based on the least square (LS) method. However, when finding the model coefficients matrix inversion is needed, which is prone to numerical instability problem [76, 110, 111]. This results in inaccurate system modelling and thereby severely degrades the performance of nonlinearity mitigation. Compared with single carrier modulation, the nonlinearity is a more serious issue for optical-OFDM due to the inherent high peak-to-average-power (PAPR) ratio of OFDM signals. Moreover, the nonlinearity also causes subcarrier interference [112]. It is shown in [35] that single carrier system (e.g., with L-ary PAM) delivers better performance than OFDM. It is worth highlighting that, single carrier system with frequency domain equalization has the same complexity with OFDM system in detection. Hence, in this Chapter, we focus on single carrier system with PAM rather than OFDM system.

In this Chapter, an alternative LED nonlinearity modelling technique based on orthogonal polynomials is investigated. As pulse amplitude modulation is often used for single-carrier LED communications, we design orthogonal polynomials for L-PAM LED signals. Although orthogonal polynomial based techniques have been investigated for power amplifier modelling and pre-distorter design, it can be only used for Gaussian distributed input signals and finding orthogonal basis for specific input distribution is difficult in general. In this work, it is the first time to apply orthogonal polynomial based technique to LED nonlinearity modelling where the input signals are real and non-negative. We developed a set of orthogonal polynomial basis for PAM LED signals for

effective system modelling. Thanks to the use of orthogonal polynomials, the columns of the basis matrix for our new model are quasi-orthogonal, so the problem of numerical instability in finding the model coefficients is avoided, leading to accurate LED nonlinearity modelling. Furthermore, a pre-distorter that has the inverse characteristic of the nonlinear model is employed to mitigate the LED nonlinearity. Simulations show that, compared to the conventional memory polynomial based technique, our proposed orthogonal polynomial based techniques can significantly reduce the nonlinear distortion and remarkable system performance improvement can be achieved.

The organization of this Chapter is as follows. In Section 3.2, the conventional memory polynomial technique is introduced. In Section 3.3, the orthogonal memory polynomial for LED nonlinearity modelling is proposed and the orthogonal polynomial basis is derived, and then, a polynomial linearization technique is presented in Section 3.4. Simulation results are provided in Section 3.5 to verify the effectiveness of our proposed method. The Chapter is concluded in Section 3.6.

3.2 Conventional Memory Polynomial Based LED Nonlinearity Modelling

Memory polynomial proposed by Kim[72] and Ding[103] is one of the most popular methods for nonlinear system modelling and pre-distortion[82]. The memory polynomial model can be expressed as

$$z(n) = \sum_{k=1}^{K} \sum_{m=0}^{M} a_{k,m} x(n-m)|x(n-m)|^{k-1}, \tag{3.1}$$

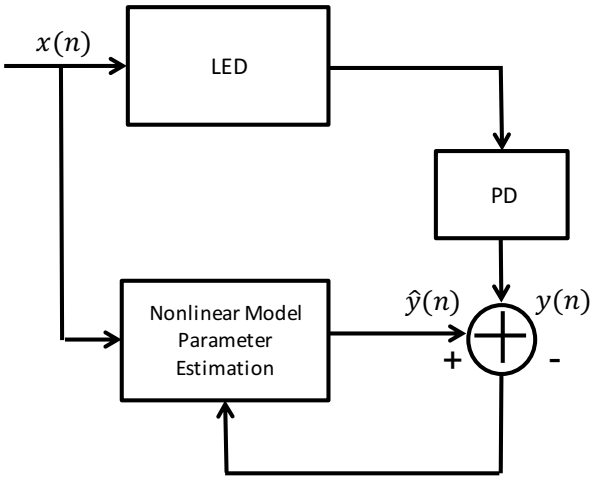

Figure 3.1: LED Nonlinearity modelling.

where $x(n)$ is the input signal, K is the order of the polynomials, M is the memory length, and $\{a_{km}\}$ are two dimensional coefficients that represent both the nonlinearity and memory effects. Noting that $x(n) \geq 0$ in LED communications, we have

$$z(n) = \sum_{k=1}^{K} \sum_{m=0}^{M} a_{k,m} x(n-m)^k \tag{3.2}$$

which can be rewritten as the following matrix form

$$\mathbf{z} = \mathbf{\Phi a} \tag{3.3}$$

where $\mathbf{z}=[z(M), z(M+1), \ldots z(N)]^T$, $\mathbf{a} = [a_{1,0}, \ldots a_{K,0}, \ldots a_{1,M}, \ldots a_{K,M}]^T$, and $\mathbf{\Phi}=[\mathbf{\Phi}_0^1, \ldots, \mathbf{\Phi}_0^K, \ldots, \mathbf{\Phi}_m^1, \ldots, \mathbf{\Phi}_m^K, \ldots, \mathbf{\Phi}_M^1, \ldots, \mathbf{\Phi}_M^K]$ with $\mathbf{\Phi}_m^k=[x(M-m)^k, x(M+1-m)^k, \ldots, x(N-m)^k]^T$.

Fig.3.1 illustrates the LED nonlinearity modelling. The electrical signal $x(n)$ is input to LED for light intensity modulation. According to the memory polynomial model in (3.1), signal $y(n)$ is linear with the polynomial coefficients to be determined. Hence, with a training sequence $\{x(n)\}$, the coefficient $\{a_{k,m}\}$ can be estimated by using the least-

squares (LS) method with the following model

$$\mathbf{y} = \mathbf{\Phi a} + \mathbf{n} \tag{3.4}$$

where $\mathbf{y}$=$[y(M), y(M+1), \ldots y(N)]^T$, and $\mathbf{n}$ represents nonlinearity modelling error and measurement noise. The LS estimate for the model coefficients is given by [110],

$$\mathbf{a} = (\mathbf{\Phi}^H \mathbf{\Phi})^{-1} \mathbf{\Phi}^H \mathbf{y}. \tag{3.5}$$

The coefficients may also be calculated and updated by using the recursive least squares (RLS) as in [109]. It has been shown that $\mathbf{\Phi}^H\mathbf{\Phi}$ is often ill-conditioned, which causes numerical instability and noise enhancement with LS estimation in (3.4) [76, 110, 111]. The problem deteriorates with the increase of K and M, and even for small values of K and M, the error induced by the matrix inversion can still be significant, leading to severe performance degradation in LED nonlinearity modelling[110], which is also demonstrated in Section 3.5 of this Chapter.

3.3 Orthogonal Polynomial Based LED Nonlinearity Modelling

To circumvent the problem of numerical instability in the above conventional memory polynomial techniques, we propose to use orthogonal polynomials for LED nonlinearity modelling. Instead of using (3.4), we use

$$\mathbf{y} = \mathbf{\Psi b} + \mathbf{n}. \tag{3.6}$$

In model (3.6), the new basis matrix $\mathbf{\Psi}$ spans the same space as $\mathbf{\Phi}$ in (3.3), and it is given by $\mathbf{\Psi} = [\mathbf{\Psi}_0^1, \ldots, \mathbf{\Psi}_0^K, \ldots, \mathbf{\Psi}_m^1, \ldots, \mathbf{\Psi}_m^K, \ldots, \mathbf{\Psi}_M^1, \ldots, \mathbf{\Psi}_M^K]$ where $\mathbf{\Psi}_m^k = [\Psi^k(x(M - m)), \Psi^k(x(M + 1 - m)), \ldots, \Psi^k(x(N - m))]^T$ and the polynomial $\Psi^k(x)$ is defined as

$$\Psi^k(x) = d_{k,k}x^k + d_{k,k-1}x^{k-1} + \cdots + d_{k,1}x \tag{3.7}$$

(here we abuse the use of superscript "k" of $\Psi^k(x)$, where k represents the order of the polynomial, rather than its power). The LS solution to (3.6) is given by

$$\mathbf{b} = (\mathbf{\Psi}^H\mathbf{\Psi})^{-1}\mathbf{\Psi}^H\mathbf{y}. \tag{3.8}$$

The above solution still involves a matrix inversion operation. To avoid the numerical instability problem, we require that any two columns of matrix $\mathbf{\Psi}$ are quasi-orthogonal. This may be achieved by properly choosing the values of the polynomial coefficients $\{d_{k,l}\}$ so that

$$E[\Psi^{k^*}(x)\Psi^l(x)] = 0, \quad k \neq l \tag{3.9}$$

i.e.,$\{\Psi^k(x)\}$ are orthogonal polynomials [110]. The values of the polynomial coefficients $\{d_{k,l}\}$ depend on the distribution of x. There are a few special orthogonal polynomials for some distributions, e.g., *Hermite* Polynomials for real valued Gaussian process with zero mean and unit variance [111]. PAM modulation is an alternative to O-OFDM for LED communications, which can be applied with orthogonal polynomials to achieve effective nonlinearity modelling. However, there are no existing orthogonal polynomials for non-negative and real-valued signal x in LED communications. In the next, we investigate the orthogonal polynomials for L-PAM LED signals.

We take 4-PAM modulation with memory polynomial of order 3 and memory length 1 as example. For a length-N training sequence, the matrix $\mathbf{\Psi}$ will be

$$\mathbf{\Psi} = \underbrace{\begin{bmatrix} \Psi^1(x(1)) & \Psi^2(x(1)) & \Psi^3(x(1)) \\ \vdots & \vdots & \vdots \\ \Psi^1(x(N)) & \Psi^2(x(N)) & \Psi^3(x(N)) \end{bmatrix}}_{\mathbf{\Psi}_0} \underbrace{\begin{bmatrix} \Psi^1(x(0)) & \Psi^2(x(0)) & \Psi^3(x(0)) \\ \vdots & \vdots & \vdots \\ \Psi^1(x(N-1)) & \Psi^2(x(N-1)) & \Psi^3(x(N-1)) \end{bmatrix}}_{\mathbf{\Psi}_1}. \tag{3.10}$$

We need to find the coefficients of the following polynomials

$$\Psi^1(x) = d_{1,1}x \tag{3.11}$$

$$\Psi^2(x) = d_{2,2}x^2 + d_{2,1}x \tag{3.12}$$

$$\Psi^3(x) = d_{3,3}x^3 + d_{3,2}x^2 + d_{3,1}x \tag{3.13}$$

where we have 6 unknown coefficients in total. Define $\alpha = \{\alpha_i, i = 1, 2, 3, 4\}$ as the alphabet of the 4-PAM modulation. It is reasonable to assume that the probabilities of $x(n) = \alpha_i$ for $i = 1, 2, 3, 4$ are the same. Hence to ensure that the first 3 columns of $\mathbf{\Psi}$ (i.e., $\mathbf{\Psi}_0$ in (3.10)) are quasi-orthogonal (the memory effects are not considered), we have the following 6 constraints

$$\sum_{i=1}^{4} \Psi^k(\alpha_i)\Psi^l(\alpha_i) = \begin{cases} 0 & if\ k \neq l \\ 1 & if\ k = l \end{cases} \tag{3.14}$$

where $k = 1, 2, 3$, and $l = 1, 2, 3$. The above 6 constraints lead to 6 second order equations with 6 unknowns, which can be solved by using the *fsolve* function in Matlab. It is

noted that, as the PAM alphabet is known, the determination of the unknown orthogonal polynomial coefficients can be carried out offline and they only need to be calculated once.

Considering memory affects, we need to take into account the last 3 columns of $\mathbf{\Psi}$, i.e., $\mathbf{\Psi}_1$ in (3.10). The use of the orthogonal polynomials guarantees that any two different column vectors in $\mathbf{\Psi}_0$ or any two different column vectors in $\mathbf{\Psi}_1$ are quasi-orthogonal. In addition, we still needs the quasi-orthogonality between any two column vectors, one from $\mathbf{\Psi}_0$ and the other one from $\mathbf{\Psi}_1$. However, our finding is that the first column in $\mathbf{\Psi}_0$ (denoted by $\mathbf{\Psi}_0^1$) and the first column in $\mathbf{\Psi}_1$ (denoted by $\mathbf{\Psi}_1^1$) can be highly correlated. This issue is unique to LED input signal which must be non-negative valued, so that all the elements in the first order vectors $\mathbf{\Psi}_0^1$ and $\mathbf{\Psi}_1^1$ have the same signs (please refer to equation (5.4)). The high correlation between $\mathbf{\Psi}_0^1$ and $\mathbf{\Psi}_1^1$ needs to be addressed, otherwise it will still cause ill condition of matrix $\mathbf{\Psi}^H\mathbf{\Psi}$, thereby resulting in numerical instability and noise enhancement in the LS estimation in (3.8). To avoid the issue, we remove the first order vector $\mathbf{\Psi}_1^1$ from $\mathbf{\Psi}$, leading to a new basis matrix $\mathbf{\Psi}'$. It is interesting that model (3.3) can still be represented by using the new basis matrix $\mathbf{\Psi}'$ as revealed by Proposition 1 and its extension. For simplicity, we only consider 4-PAM signalling and nonlinear model with polynomial order 4 and memory length 1 in the above. The discussions can be extended to any PAM signalling and nonlinear models with different polynomial orders and memory lengths.

Proposition 1: For non-negative L-PAM with $L = K$, model (3.3) can be represented by using the orthogonal polynomial based basis matrix $\mathbf{\Psi}'$ which is constructed from $\mathbf{\Psi}$ by removing its first order columns for memory parts, i.e., there always exists $\mathbf{b}'$ so that

$\mathbf{\Psi}'\mathbf{b}'=\mathbf{\Phi}\mathbf{a}$.

Proof: Without loss of generality, consider 4-PAM signalling, and assume that the nonlinear model has polynomial of order 4 and memory length 2. According to (3.2) (which is equivalent to (3.3)),

$$y_c(n) = \sum_{k=1}^{4} a_{k,0}x(n)^k + \sum_{k=1}^{4} a_{k,1}x(n-1)^k + \sum_{k=1}^{4} a_{k,2}x(n-2)^k. \tag{3.15}$$

The orthogonal polynomial model with basis matrix $\mathbf{\Psi}'$ is given by

$$y_o(n) = \sum_{k=1}^{4} b_{k,0}\Psi^k(x(n)) + \sum_{k=2}^{4} b_{k,1}\Psi^k(x(n-1)) + \sum_{k=2}^{4} b_{k,2}\Psi^k(x(n-2)) \tag{3.16}$$

where $\{\Psi^k(x(n))\}$ are orthogonal polynomials, and the polynomial coefficients are determined as shown in Section 3. Next, we prove that, there exist $\{b_{k,l}\}$ which make the two models (3.15) and (3.16) equivalent. The elements of the 4-PAM alphabet are denoted by α_1, α_2, α_3 and α_4. Define

$$P_{c_0}(x) = \sum_{k=1}^{4} a_{k,0}x^k, \quad A_{0,i} = P_{c_0}(\alpha_i)$$

$$P_{c_1}(x) = \sum_{k=1}^{4} a_{k,1}x^k, \quad A_{1,i} = P_{c_1}(\alpha_i)$$

$$P_{c_2}(x) = \sum_{k=1}^{4} a_{k,2}x^k, \quad A_{2,i} = P_{c_2}(\alpha_i)$$

$$P_{o_0}(x) = \sum_{k=1}^{4} b_{k,0}\Psi^k(x), \quad B_{0,i} = P_{o_0}(\alpha_i)$$

$$P_{o_1}(x) = \sum_{k=2}^{4} b_{k,1}\Psi^k(x), \quad B_{1,i} = P_{o_1}(\alpha_i)$$

$$P_{o_2}(x) = \sum_{k=2}^{4} b_{k,2}\Psi^k(x), \quad B_{2,i} = P_{o_2}(\alpha_i).$$

Then equations (3.15) and (3.16) can be rewritten as

$$y_c(n) = A_{0,r} + A_{1,s} + A_{2,t}, \quad r, s, t = 1, 2, 3, 4, \tag{3.17}$$

$$y_o(n) = B_{0,r} + B_{1,s} + B_{2,t}, \quad r, s, t = 1, 2, 3, 4. \tag{3.18}$$

As we are considering 4-PAM, each term in (3.17) or (3.18) has 4 values, so there are 64 combinations. It appears that we need 64 equations to make (3.17) and (3.18)

equivalent. In fact, these 64 equations can be reduced to the following 10 equations.

$$A_{01} + A_{11} + A_{21} = B_{01} + B_{11} + B_{21} \tag{3.19}$$

$$A_{02} + A_{12} + A_{22} = B_{02} + B_{12} + B_{22} \tag{3.20}$$

$$A_{03} + A_{13} + A_{23} = B_{03} + B_{13} + B_{23} \tag{3.21}$$

$$A_{04} + A_{14} + A_{24} = B_{04} + B_{14} + B_{24} \tag{3.22}$$

$$A_{11} - A_{12} = B_{11} - B_{12} \tag{3.23}$$

$$A_{11} - A_{13} = B_{11} - B_{13} \tag{3.24}$$

$$A_{11} - A_{14} = B_{11} - B_{14} \tag{3.25}$$

$$A_{21} - A_{22} = B_{21} - B_{22} \tag{3.26}$$

$$A_{21} - A_{23} = B_{21} - B_{23} \tag{3.27}$$

$$A_{21} - A_{24} = B_{21} - B_{24} \tag{3.28}$$

It can be verified that, (3.19) together with (3.23-3.28) guarantees that (3.17) and (3.18) are equal for 16 combinations i.e., $r = 1, s \in (1, 2, 3, 4)$ and $t \in (1, 2, 3, 4)$. Similarly, (3.20), (3.21) and (3.22) with (3.23-3.28) guarantee the other 48 combinations. Hence, the above 10 equations guarantee (3.17) and (3.18) are equal for all 64 combinations. As the number of unknowns $\{b_{k,l}\}$ is ten, their values can be determined. The above proof can also be extended to larger memory length and higher order polynomials.

Extension to $L > K$***:*** In the above proof, we assume that the size of the PAM alphabet L is equal to the order of the polynomial K. In the case of high order PAM, L

may be larger than K. In the following, we consider the case of $L > K$.

From (3.23-3.25), we can see that when $x = \alpha_1, \alpha_2, \alpha_3$ and α_4, $P_{c_1}(x) - P_{o_1}(x) = C_1$ where C_1 is a constant. Similarly, we can also show that when $x = \alpha_1, \alpha_2, \alpha_3$ and α_4, $P_{c_0}(x) - P_{o_0}(x) = C_0$ and $P_{c_2}(x) - P_{o_2}(x) = C_2$. Because (3.17) is equivalent to (3.18), $C_0 + C_1 + C_2 = 0$. When $L > K$, we can select K elements α_1, α_2, α_3, ... α_K from the L-PAM alphabet. Similar to the proof in Proposition 1, we have $P_{c_0}(x) - P_{o_0}(x) = C_0$, $P_{c_1}(x) - P_{o_1}(x) = C_1$, $P_{c_2}(x) - P_{o_2}(x) = C_2$ and $C_0 + C_1 + C_2 = 0$ when x=α_1, α_2, α_3, ... α_K.

According to [113], we have

$$P_{c_0}(x) = \Delta_0 P_{c_0}(0) + \Delta_1 P_{c_0}(\alpha_1) + ... + \Delta_k P_{c_0}(\alpha_K) = \sum_{i=0}^{K} \Delta_i P_{c_0}(\alpha_i) \tag{3.29}$$

$$P_{o_0}(x) = \Delta_0 P_{o_0}(0) + \Delta_1 P_{o_0}(\alpha_1) + ... + \Delta_k P_{o_0}(\alpha_K) = \sum_{i=0}^{K} \Delta_i P_{o_0}(\alpha_i) \tag{3.30}$$

where

$$\Delta_i = \prod_{j=0,\ j\neq i}^{K} \frac{x - \alpha_j}{\alpha_i - \alpha_j}$$

with $\alpha_0 = 0$. Then, we define

$$h_0(x) = P_{c_0}(x) - P_{o_0}(x) = \sum_{i=0}^{K} \Delta_i (P_{c_0}(\alpha_i) - P_{o_0}(\alpha_i)) = \sum_{i=0}^{K} \Delta_i C_0. \tag{3.31}$$

For LED communications, the input voltage x is approximately within the range of 2.4v-3.8v [114]. Next, we show that when x∈[2.4,3.8], $h_0(x)$ is still approximately a constant C_0. We can select the following K elements from [2.4,3.8] as $\alpha_1 = 2.4$, $\alpha_2 = \alpha_1 + 1.4\frac{1}{K-1}$,

$\alpha_3 = \alpha_1 + 1.4\frac{2}{K-1}$, ..., $\alpha_K = 3.8$. When $K = 4$, we have

$$h_0(x) = (-0.0115x^4 + 0.1423x^3 - 0.6554x^2 + 1.3287x)C_0 = g_0(x)C_0. \tag{3.32}$$

It is not hard to show that the maximum value and minimum value of $g_0(x)$ with $x\in[2.4,3.8]$ are 1.0005 and 0.9997, respectively. Hence, $h_0(x)$ is between $0.9997C_0$ and $1.0005C_0$, i.e., $h_0(x) = P_{c_0}(x) - P_{o_0}(x) \approx C_0$ when $x\in[2.4,3.8]$. When $K = 5$, we can find that $h_0(x)$ is between $0.9999C_0$ and $1.0001C_0$. We can see that, with the increase of K, $h_0(x)$ approaches to C_0 more accurately. Similarly, we have $P_{c_1}(x) - P_{o_1}(x) \approx C_1$ and $P_{c_2}(x) - P_{o_2}(x) \approx C_2$ when $x\in[2.4,3.8]$. Therefore, $\mathbf{\Psi}'\mathbf{b}'\approx\mathbf{\Phi a}$ for any x within the LED input voltage range. So, $\mathbf{\Psi}'\mathbf{b}'\approx\mathbf{\Phi a}$ for L-PAM with $L > K$.

The first order columns of $\mathbf{\Psi}$ in the memory part $\mathbf{\Psi}_M^1(m \neq 0)$ are removed, forming a new matrix $\mathbf{\Psi}'$, so that the columns of $\mathbf{\Psi}'$ can be quasi-orthogonal, by properly choosing the values of the polynomial coefficients $\{d_{\{k,l\}}\}$. This leads to

$$\mathbf{y} = \mathbf{\Psi}'\mathbf{b}' + \mathbf{n}. \tag{3.33}$$

With the new basis matrix $\mathbf{\Psi}'$, the numeric instability problem can be avoided, which is crucial to achieve accurate LED nonlinearity modelling, as demonstrated in Section 5. Based on the orthogonal polynomial basis $\mathbf{\Psi}'$, we can get the LS solution to (3.33)

$$\mathbf{b}' = (\mathbf{\Psi}'^H\mathbf{\Psi}')^{-1}\mathbf{\Psi}'\mathbf{y}. \tag{3.34}$$

Although the above solution still involves a matrix inverse operation, the numerical instability problem is avoided due to the quasi-orthogonality of $\mathbf{\Psi}'$ [76]. Then, the nonlinear

LED model (3.10) can be obtained because $\mathbf{\Psi}'\mathbf{b}' \approx \mathbf{\Phi}\mathbf{a}$.

3.4 LED Nonlinearity Mitigation through Pre-distortion

As shown in Fig. 3.2, once the nonlinear model for LED is found, a straightforward method for nonlinearity mitigation is to use a pre-distorter (at the transmitter) which is an inverse function of the obtained nonlinear model [57]. With the use of the pre-distorter, the output of the LED,

$$y(n) = ax(n) + b \tag{3.35}$$

where a and b are two constants which can be determined with the nonlinear model as shown in Fig. 3.3. The polynomian linearization technique is illustrated in Fig. 3.3 where the memory effects are not considered. For an input x, the output of the LED should be y. As the nonlinear model is known, we can find x' as shown in Fig. 3.3. Actually, no inverse function is attained, the task of the pre-distorter is to shift x to x' according to the shifting rules defined in Fig. 3.3. When the memory effects are considered, we rewrite the nonlinear equation as

$$y(n) = \sum_{k=1}^{K} a_{k,0} x'(n)^k + \underbrace{\sum_{k=1}^{K} \sum_{m=1}^{M-1} a_{k,m} x'(n-m)^k}_{p(n)} = ax(n) + b. \tag{3.36}$$

The first term represents the non-memory part while the second part represents the memory part. It is noted that, at time instant n, $\{x'(n-m), m = 1, \ldots, M-1\}$ are known, so the second term $p(n)$ in the above equation can be calculated and cancelled. Hence, we

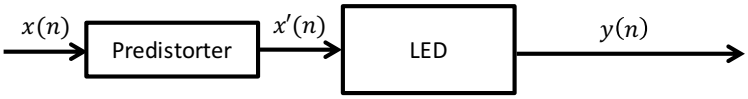

Figure 3.2: Block diagram of pre-distortion.

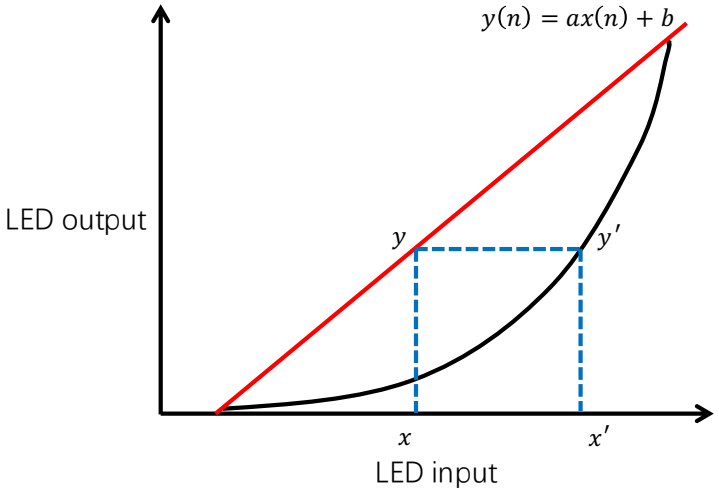

Figure 3.3: Illustration of polynomial linearization technique (without considering memory effects).

have

$$y^{'}(n) = ax(n) + b - p(n) = \sum_{k=1}^{K} a_{k,0} x^{'}(n)^{k}. \tag{3.37}$$

Then the memory case is reduced to the memoryless case and $x'(n)$ can be found. [a]

3.5 Simulation Results

In this section, we compare the performance of the conventional polynomial technique and the proposed orthogonal polynomial technique in terms of LED nonlinearity modelling error and symbol error rate (SER) of the LED communication. We assume that the memory length is 1. The LED nonlinear transfer function is given by Hammerstein

[a] In order to avoid the case that $x'(n)$ is smaller than the turn-on voltage, we need $ax(n) + b - p(n) > 0$, which can be satisfied by properly choosing the values of a and b.

Table 3.1: Orthogonal polynomial basis for 4-PAM with K=4.

$\Psi^1(x)$	$0.150142 \times x$
$\Psi^2(x)$	$0.341963 \times x^2 - 1.150401 \times x$
$\Psi^3(x)$	$0.960947 \times x^3 - 6.417431 \times x^2$ $+10.525301 \times x$
$\Psi^4(x)$	$3.565086 \times x^4 - 35.452668 \times x^2$ $+116.356321 \times x^2 - 125.983919 \times x$

model[115]

$$z(n) = \sum_{k=1}^{K} a_k x(n)^k + \lambda(\sum_{k=1}^{K} a_k x(n-1)^k) \tag{3.38}$$

where the gain of the memory effect $\lambda = 0.1$, and the polynomial coefficients $\{a_k\}$ are obtained based on a LED data sheet [114]. We choose $K = 4$ and 5, and the coefficients are $a_1 = 34.11$, $a_2 = -29.99$, $a_3 = 6.999$, $a_4 = -0.1468$ for $K = 4$ and they are $a_1 = 413.2$, $a_2 = -541.5$, $a_3 = 263.4$, $a_4 = -56.73$, $a_5 = 4.639$ for $K = 5$.

We develop the orthogonal polynomials for LED communications with 4-PAM signalling and 8-PAM signalling which can be used to achieve higher data bit rate. Considering 4-PAM modulation and we choose the LED input voltage $x\in$[2.5, 2.9, 3.3, 3.7] and 8-PAM with the input voltage $x\in$[2.4, 2.6, 2.8, 3.0, 3.2, 3.4, 3.6, 3.8] as the PAM alphabets, respectively. The orthogonal polynomial basis we developed are shown in Table. 3.1 and Table. 3.2 for reference.

The parameters of the nonlinear model are estimated using training sequence with LS. To evaluate the modelling performance, we define the normalized mean square error

Table 3.2: Orthogonal polynomial basis for 8-PAM with K=4.

$\Psi^1(x)$	$0.109369 \times x$
$\Psi^2(x)$	$0.246617 \times x^2 - 0.820892 \times x$
$\Psi^3(x)$	$0.613158 \times x^3 - 3.987077 \times x^2$ $+6.357259 \times x$
$\Psi^4(x)$	$1.627234 \times x^4 - 15.767919 \times x^2$ $+50.335199 \times x^2 - 52.900603 \times x$
$\Psi^5(x)$	$-5.606703 \times x^5 + 72.183027 \times x^4$ $-345.637522 \times x^3 + 729.347864 \times x^2$ $-572.135152 \times x$

(NMSE) as

$$nmse(dB) = 10 \log 10[\frac{\sum_{n=1}^{N} |y(n) - \hat{y}(n)|^2}{\sum_{n=1}^{N} |y(n)|^2}] \tag{3.39}$$

where $y(n)$ is LED output and $\hat{y}(n)$ is the output of our nonlinear modeller as shown in Fig. 3.4. The input $\{x(n)\}$ are randomly generated 4-PAM and 8-PAM signals. The channel is being considered as a line of sight channel and additive white Gaussian noise (AWGN) is added at the receiver side. The variance of the measurement noise in (3.4) and (3.6) is denoted by σ_n^2. We define the SNR in nonlinearity modelling as $SNR = E(z(n)^2)/\sigma_n^2$, where $z(n)$ is given in (3.2).

Table 3.3 shows the results of system modelling with 4-PAM. It can be seen that the conventional polynomial based technique does not work. It is also noted that the orthogonal polynomial based technique with basis $\mathbf{\Psi}$ performs poorly because it still suffers from the ill-condition matrix inversion problem as discussed in Section 3. In contrast,

Table 3.3: Modelling error (NMSE in db) with 4-PAM where modelling SNR=30dB and K=4.

	conventional polynomial	orthogonal polynomial with $\mathbf{\Psi}$	orthogonal polynomial with $\mathbf{\Psi}'$
Training length 100	121.9389	26.0605	-26.9156
Training length 300	121.3331	25.8536	-31.6447
Training length 500	120.3250	25.6039	-33.9727

Table 3.4: Modelling error (NMSE in db) with 8-PAM where modelling SNR=30dB and K=4.

	conventional polynomial	orthogonal polynomial (proposed)
Training length 100	-21.7128	-26.6246
Training length 300	-24.2907	-31.1429
Training length 500	-24.7386	-33.5791

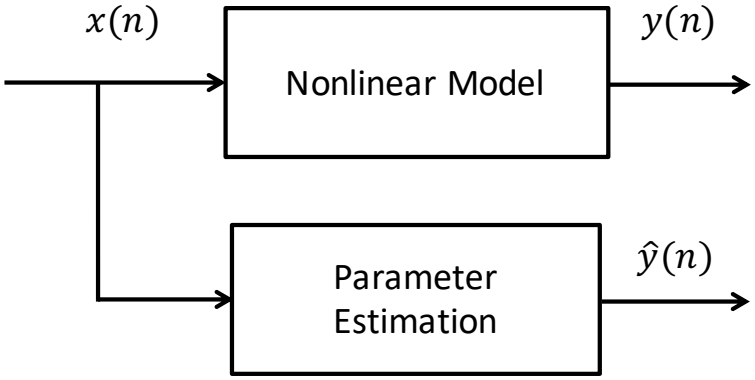

Figure 3.4: Definition of NMSE.

Table 3.5: Modelling error (NMSE in db) with 8-PAM where modelling SNR=30dB and K=5.

	conventional polynomial	orthogonal polynomial (proposed)
Training length 100	73.7229	-25.1126
Training length 300	72.8256	-29.8513
Training length 500	72.9188	-32.0913

the proposed technique with basis $\mathbf{\Psi}'$ works very well. In the subsequent simulations, orthogonal polynomial technique with basis $\mathbf{\Psi}$ will not be considered. Tables 3.4 and 3.5 show the results of system modelling with 8-PAM of order $K = 4$ and $K = 5$, respectively. It can be seen that our proposed method achieves much better performance than the conventional one. With longer training sequence, better performance can be obtained. We note that the conventional technique suffers from the numerical instability problem when the order $K = 4$ and even does not work when the order of the polynomial $K = 5$.

Figures 3.5 and 3.6 show the SER performance of the LED system with the pre-

distorter designed in Section 3.4, where the polynomial coefficients are obtained using the conventional and proposed techniques with training sequence of length 500. The SNR for SER simulation is defined as $SNR = E(y(n)^2)/\sigma_w^2$, where $y(n)$ is shown in Fig. 3.2 and σ_w^2 is the variance of the AWGN. The performance of the system without nonlinear distortion is also shown in Figs. 3.5 and 3.6 for reference, which is the lower bound of the SER performance. It can be seen from Fig. 3.5 (where $K = 4$) that both techniques work, but the proposed one outperforms the conventional one, especially when SNR is high. We can still see a small gap between the proposed technique and the lower bound, which is due to the residual nonlinear distortion. In Fig. 3.6 (where $K = 5$), the conventional technique does not work due to severe ill-condition of the matrix inversion. However, the proposed one still works well and the performance is very close to the lower bound. The reason is that significant errors are induced due to the problem of numerical instability of matrix inversion. In contrast, our approach works very well thanks to the use of orthogonal polynomials. Accurate nonlinearity modelling leads to high overall system SER performance. Figures 3.7 and 3.8 show the performance of different techniques in terms of error vector magnitude (EVM) [109]. Figures 3.7 and 3.8 have the same simulation settings as Figs. 3.5 and 3.6, respectively. The results again demonstrate the advantage of our proposed orthogonal polynomial technique.

3.6 Conclusion

In this Chapter, we have investigated LED nonlinearity modelling and mitigation technique for LED communications with PAM signalling. An orthogonal polynomial based

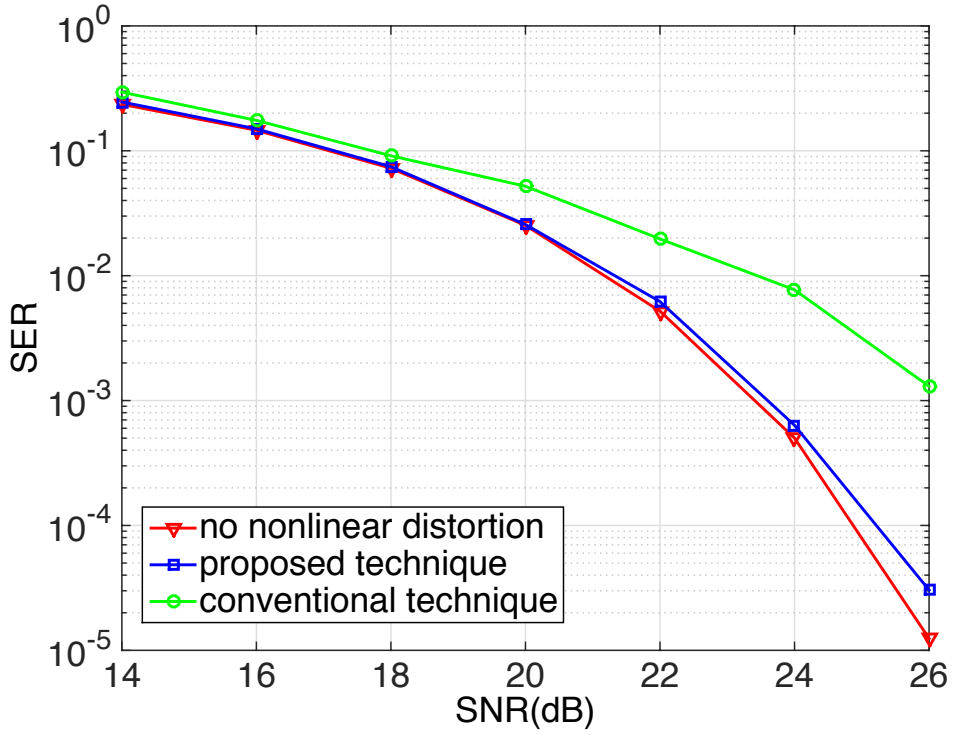

Figure 3.5: SER performance comparison with 8-PAM and K=4.

technique has been proposed for real-valued non-negative LED signals to achieve accurate LED nonlinearity modelling by avoiding the numerical instability of the conventional techniques. Furthermore, a pre-distorter is employed to mitigate the LED nonlinearity with memory effects. It is shown that the proposed technique significantly outperforms the conventional technique in terms of LED nonlinearity modelling error and system SER performance.

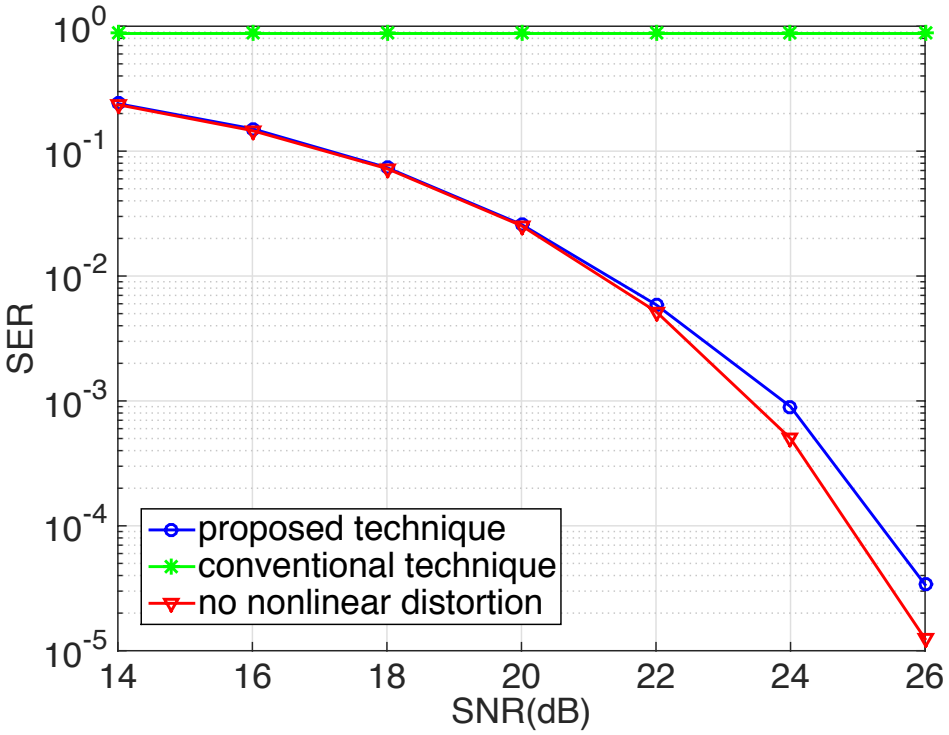

Figure 3.6: SER performance comparison with 8-PAM and K=5.

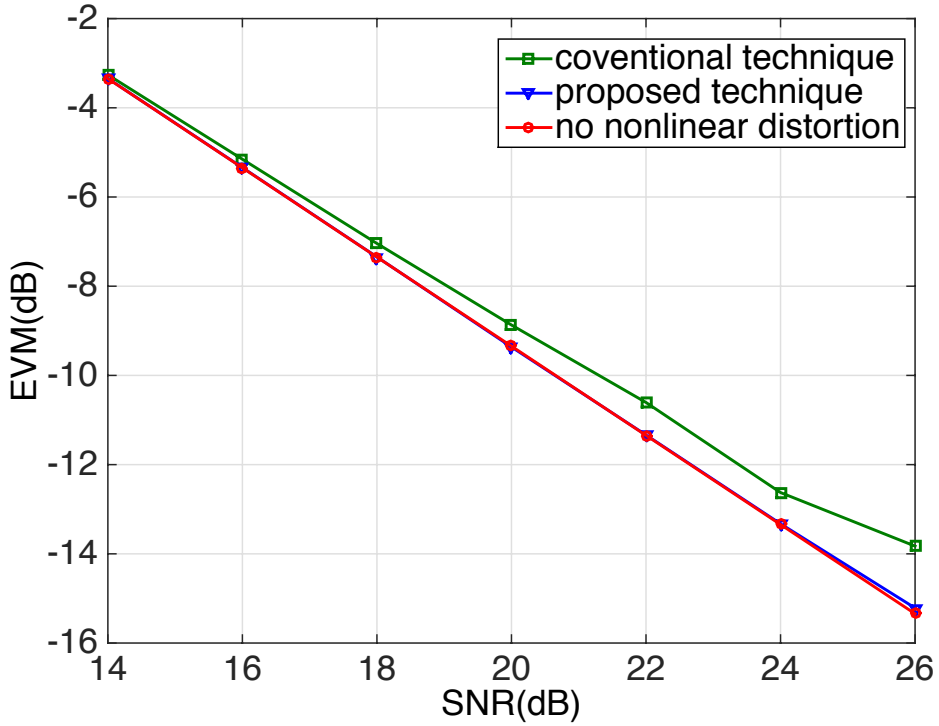

Figure 3.7: EVM performance comparison with 8-PAM and K=4.

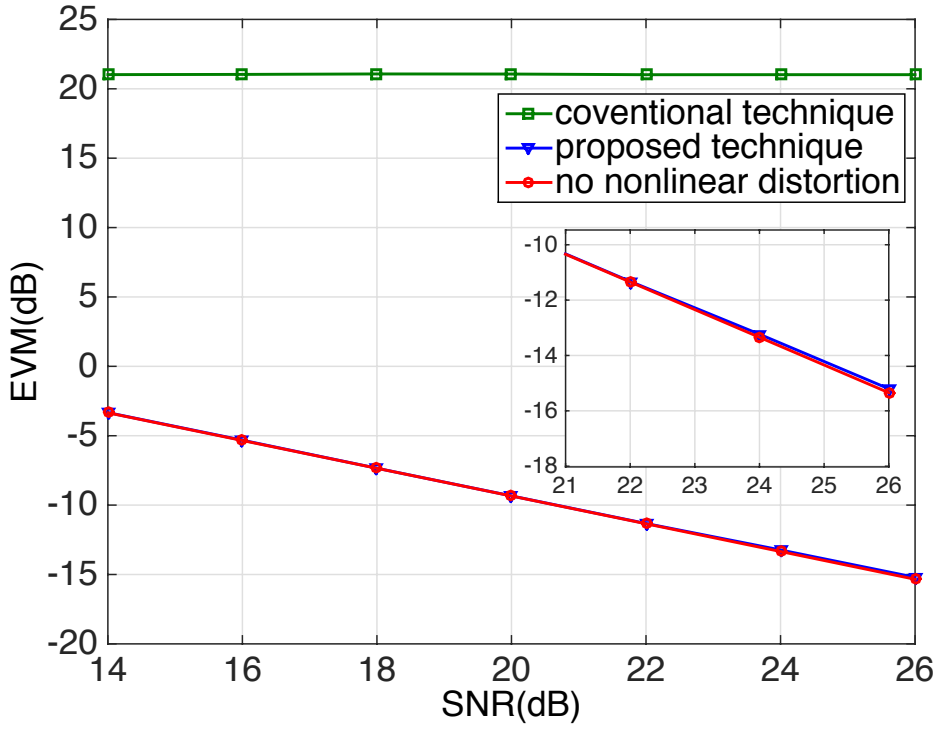

Figure 3.8: EVM performance comparison with 8-PAM and K=5.

Chapter 4

Frequency Domain Equalization and Post-distortion for LED Communications with Orthogonal Polynomial Based Joint LED Nonlinearity and Channel Estimation

4.1 Introduction

The nonlinearity of LED is a challenge in LED communications, and it needs to be effectively modelled and then mitigated to avoid system degradation due to nonlinear distortion. Additionally, in indoor optical wireless communication environment, optical detectors may receive signals propagated from emitters through multiple paths due to reflections of room surfaces or other objects [116]. The multipath propagation includes

two types: line of sight (LOS) propagation which depends on the distance and orientation between emitter and receiver, and non-LOS which is also known as diffuse link due to reflections off the room surroundings. Such multipath dispersion can lead to inter-symbol interference (ISI) at high data rates [117].

Therefore, LED Nonlinearity and channel modelling and mitigation are vital for LED communications to avoid system performance degradation. In Chapter 3, we proposed an orthogonal polynomial-based LED nonlinearity modelling technique [118]. We built a set of orthogonal polynomial basis for PAM modulated LED signals to accomplish effective LED nonlinearity modelling. Due to the use of orthogonal polynomials, the basis matrix for our new model are quasi-orthogonal (leading to low complexity inversion of the corresponding correlation matrix), so the problem of numerical instability in doing the matrix inverse operation is solved, resulting in accurate LED nonlinearity modelling and significantly better performance. In the above works, only LOS channels are considered; whilst the ISI effect in optical wireless communications is ignored. In [119], OFDM is used for the mitigation of ISI. However, as OFDM signals has inherent high peak-to-average-power (PAPR) ratio [120], the LED nonlinearity is a more serious issue. In [121], single carrier modulation with frequency domain equalization (FDE) is used to combat ISI in LED communications. However, the nonlinear distortion in LEDs is not considered.

In this Chapter, we will first extend our previous work on orthogonal polynomial based LED modelling [118] and demonstrate another advantage of this approach, i.e., it allows the simultaneous estimation of the LED nonlinearity and ISI channel coefficients. According to [122] and [123], the bandwidth limitation of LED induced fading will also affect the system performance. In this work, we consider both the LED nonlinearity

and LED memory effect. We develop a joint estimation approach for LED nonlinearity and composite ISI channel. The orthogonal polynomial based joint estimation technique circumvents the numerical instability problem over the traditional one and it has low complexity thanks to the orthogonal property of the basis matrix. It is shown in [35] that single carrier LED communication systems can deliver better performance than OFDM LED systems, but conventional single carrier systems require higher computational complexity compared to OFDM ones. It is worth emphasizing that, single carrier system with FDE has similar complexity as OFDM one. Hence, in this work, the ISI effect due to the LED and channel memory is eliminated through frequency domain equalization. Moreover, a post-distorter is employed to mitigate memoryless LED nonlinearity. To the best of our knowledge, for the first time, both LED nonlinearity with memory effect and ISI optical channel are jointly estimated and mitigated. Our work shows that the proposed technique can effectively mitigate the nonlinearity and ISI distortion and significant system performance improvement can be achieved.

The organization of this Chapter is as follows. In Section 4.2, optical wireless channel model is given, and the receiver design for joint LED nonlinearity and ISI channel estimation and mitigation is detailed. Simulation results are provided in Section 4.3 to verify the effectiveness of our proposed technique. The Chapter is concluded in Section 4.4.

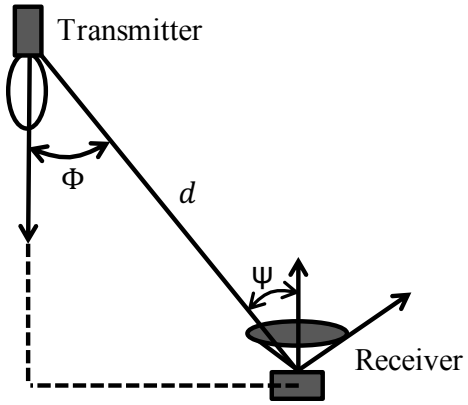

Figure 4.1: LOS propagation.

4.2 Equalization and Post-distortion with Orthogonal Polynomial Based Joint Nonlinearity and Channel Estimation

4.2.1 ISI Channel Model for Indoor LED Communications

In indoor LED communications, optical detectors may receive signals propagated from emitters through multiple paths due to reflections off the room surfaces or any other objects. The optical wireless channel transfer function is given by [124]

$$h(t) = h_{los}(t) + h_{nlos}(t), \tag{4.1}$$

where $h_{los}(t)$ is the contribution due to LOS, which is independent of the modulation frequency but depends on the distance and orientation between emitter and receiver, and $h_{nlos}(t)$ represents non-LOS propagation, which is known as diffuse link due to reflections off the room surroundings. As shown in Fig. 4.1, where we consider a receiver located at a distance of d and angle Φ with respect to emitter, the impulse response of LOS link

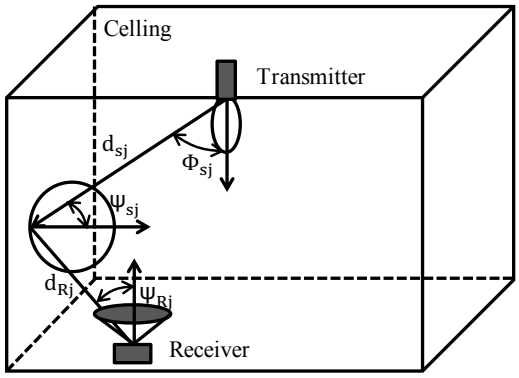

Figure 4.2: NLOS propagation.

can be expressed as [125–127]

$$h_{los}(t) = \frac{A_r}{d^2} R_0(\Phi) T_s(\Psi) g(\Psi) cos(\Psi) \delta(t - d/c), \tag{4.2}$$

where A_r is the active area of the photo-diode, $T_s(\Psi)$ is the optical band-pass filter, $g(\Psi)$ is the gain of non-imaging concentrator, c is the speed of the light in free space, δ is the Dirac function, and $R_0(\Phi)$ denotes the Lambertian radiant intensity, which is given by

$$R_0(\Phi) = \begin{cases} \frac{m_1+1}{2\pi} cos^{m_1}(\Phi) & for \ \ \Phi \in [-\pi/2, \pi/2] \\ 0 & for \ \ \Phi \geqslant \pi/2 \end{cases}, \tag{4.3}$$

where m_1 is the Lambert's mode number expressing directivity of the source beam, Φ is the angle of maximum radiated power. The order of Lambertian emission m_1 is related to the LED semi-angle at half-power $\Phi_{1/2}$ by

$$m_1 = \frac{-ln2}{ln(cos(\Phi_{1/2}))}. \tag{4.4}$$

For the non-LOS model, the surfaces of the room are divided by R reflecting elements with area of ΔA. As shown in Fig. 4.2, given a particular single source S and

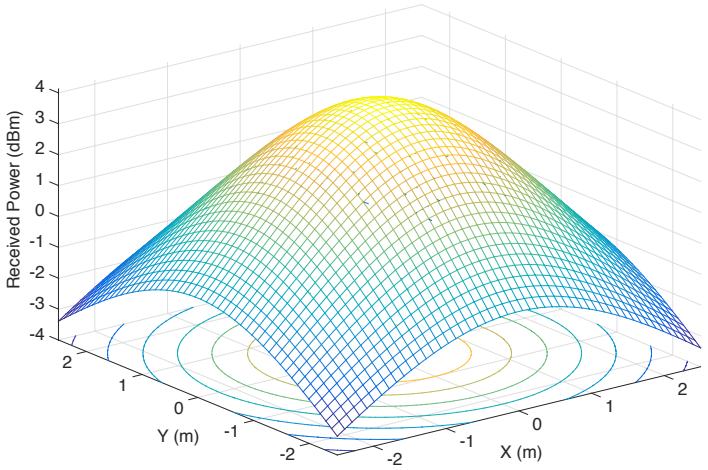

Figure 4.3: Received power distribution for LOS channel.

receiver, the channel response after one reflection can be approximated as [125–127]

$$h_{nlos}(t) = \sum_{j=1}^{R} \frac{\rho_j A_r \Delta A}{d_{sj}^2 d_{Rj}^2} R_0(\Phi_{sj}) cos(\Psi_{sj}) cos(\Psi_{Rj}) \delta(t - \frac{d_{sj} + d_{Rj}}{c}), \tag{4.5}$$

where ρ_j is the reflection coefficient of j.

Considering a room of 5×5×3 m^3 with a single light source on the centre of the celling at height 2.15m, reflection coefficient $\rho = 0.8$, LED semi-angle 70° with power 20w and field of view (FOV) of the photo detector 60°, the distribution of received power for LOS and NLOS channel are shown in Fig. 4.3 and 4.4, respectively.

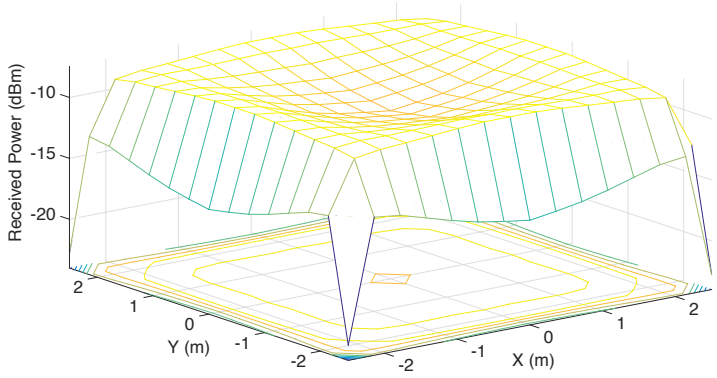

Figure 4.4: Received power distribution for NLOS channel.

4.2.2 Receiver Design

Joint LED Nonlinearity and ISI Channel Estimation

In this work, we employ the Hammerstein model for the nonlinearity and memory effect of the LED, it can be represented as [128]

$$z(n) = \sum_{m=1}^{M} b_m g(x(n-m)), \tag{4.6}$$

where $g(\cdot)$ is a memoryless polynomial and

$$g(x) = \sum_{k=1}^{K} a_k x^k. \tag{4.7}$$

After transmitting through the optical wireless channel, the received signal can be represented as

$$\mathbf{y} = \mathbf{z} * \mathbf{h} + \mathbf{n}, \tag{4.8}$$

where symbol $*$ denotes linear convolution, $\mathbf{z}=[z(M), z(M+1), \ldots z(N)]^T$ is the transmitted signal vector, $\mathbf{h} = [h_0, h_1, \ldots, h_{L-1}]^T$ is a length L vector representing the unknown optical channel taps, which can be obtained by sampling $g_{tx}(t)*h(t)*g_{rx}(t)$ with $g_{tx}(t)$ and $g_{rx}(t)$ being the transmit and receive filters, $\mathbf{y}=[y(M), y(M+1), \ldots y(N+L-1)]^T$ is the received signal vector, and $\mathbf{n}=[n(M), n(M+1), \ldots n(N+L-1)]^T$ denotes the additive white Gaussian noise (AWGN) with variance N_0.

It can be seen that the optical channel $\mathbf{h}$ can be absorbed into the Hammerstein model, so that $\mathbf{z} * \mathbf{h}$ in (4.8) can be written as

$$z^{'}(n) = \sum_{k=1}^{K} \sum_{i=0}^{L+M-1} a_k c_i x(n-i)^k, \tag{4.9}$$

where c_i is the *ith* element of the length-$(L+M-1)$ vector $\mathbf{c} = \mathbf{h}*\mathbf{b}$ and $\mathbf{c}$ is called the composite ISI channel vector. It is clear that (4.9) is a special case of the memory polynomial model with $\{a_k\}$ representing the memoryless nonlinearity coefficients and $\{c_i\}$ representing the composite ISI channel coefficients, respectively. However, due to the removal of the first order columns of the memory parts in $\mathbf{\Psi}$ (please refer to Chapter 3), we cannot obtain $\{a_k\}$ and $\{c_i\}$ directly by using our orthogonal polynomial technique. In the following, we show how to estimate the LED nonlinearity and composite ISI channel simultaneously. The technique was developed based on our work on orthogonal polynomial modelling method in Chapter 3. But it cannot be employed straightforwardly and some tricks are explained in detail.

According to (3.33), the orthogonal polynomial model with basis matrix $\mathbf{\Psi}^{'}$ can be

expressed as

$$y_o(n) = \sum_{k=1}^{K} b_{k,0}\Psi^k(x(n)) + \sum_{k=2}^{K}\sum_{i=1}^{L+M-1} b_{k,i}\Psi^k(x(n-i)). \tag{4.10}$$

With training signals at the receiver side, we can get LS estimates of $\{b_{k,i}\}$, which are two dimensional parameters that represent both the nonlinearity and composite ISI channel. A difficult is that the composite channel coefficients and the nonlinearity coefficients are tangled together in the form of multiplication. Next, we show how to seperate $\{c_i\}$ with $\{a_k\}$ from $\{b_{k,i}\}$. In Chapter 3 Section 3.3, we have proved that (4.10) and (4.9) have the following relationship

$$\sum_{k=1}^{K} a_k c_0 x(n)^k - \sum_{k=1}^{K} b_{k,0}\Psi^k(x(n)) \approx A_0, \tag{4.11}$$

$$\sum_{k=1}^{K} a_k c_i x(n-i)^k - \sum_{k=2}^{K} b_{k,i}\Psi^k(x(n-i)) \approx A_i, i \neq 0, \tag{4.12}$$

where $\{A_0, \ldots, A_i\}$ are all constants and $A_0 + \cdots + A_i \approx 0$.

In the following, we first calculate c_i and A_0 according to the above relationships based on $\{b_{k,i}\}$. Define

$$D^k = \{x_l^k - x_m^k, 1 \leq m < l \leq L\}, \tag{4.13}$$

where L is the size of the PAM alphabet and the size of set D^k is $L \times (L-1)/2$. We use D_j^k to denote the *jth* element in D^k and define

$$\Delta_D = \sum_{j=1}^{\frac{L\times(L-1)}{2}} \sum_{k=1}^{K} a_k D_j^k. \tag{4.14}$$

Similarly, define

$$E^k = \{\Psi^k(x_l) - \Psi^k(x_m), 1 \leq m < l \leq L\}, \tag{4.15}$$

where the size of set E^k is $L \times (L-1)/2$. We use E^k_j to denote the jth element in E^k and define

$$\Delta_{E_0} = \sum_{j=1}^{\frac{L\times(L-1)}{2}} \sum_{k=1}^{K} b_{k,0} E^k_j, \tag{4.16}$$

and

$$\Delta_{E_i} = \sum_{j=1}^{\frac{L\times(L-1)}{2}} \sum_{k=2}^{K} b_{k,i} E^k_j. \tag{4.17}$$

It can be seen that Δ_D, Δ_{E_0} and Δ_{E_i} depend on the PAM alphabet and they are constants when the alphabet is fixed.

Substituting different values of $x(n)$ into (4.11), we have the following for x_l and x_m $\in \chi$ $(x_l \neq x_m)$,

$$\sum_{k=1}^{K} a_k c_0 x_l^k - \sum_{k=1}^{K} a_k c_0 x_m^k \approx \sum_{k=1}^{K} b_{k,0} \Psi^k(x_l) - \sum_{k=1}^{K} b_{k,0} \Psi^k(x_m). \tag{4.18}$$

So we can have $L\times(L-1)/2$ equations for different combinations of x_l and x_m. Then, summing each side of these equations, leads to

$$c_0 \Delta_D = \Delta_{E_0}. \tag{4.19}$$

Similarly, based on (4.12), we have

$$c_i \Delta_D = \Delta_{E_i}. \tag{4.20}$$

From (4.19) and (4.20), we have the proportional relationship of the composite ISI chan-

nel coefficients

$$\frac{c_0}{c_i} = \frac{\Delta_{E_0}}{\Delta_{E_i}}, \forall i. \tag{4.21}$$

Also, adding equation (4.11) and (4.12), leads to

$$\frac{c_0}{c_i} = \frac{E_0 + LA_0}{E_i + LA_i}, \forall i, \tag{4.22}$$

where $E_0 = \sum_{k=1}^{K} \sum_{l=1}^{L} b_{k,0} \Psi^k(x_l)$ and $E_i = \sum_{k=2}^{K} \sum_{l=1}^{L} b_{k,i} \Psi^k(x_l)$, which are all known. From (4.21) and (4.22), we have

$$\frac{\Delta_{E_0}}{\Delta_{E_i}} = \frac{E_0 + LA_0}{E_i + LA_i}, i = 1, 2 \ldots, I. \tag{4.23}$$

With $A_0 + \cdots + A_i \approx 0$, A_0 can be determined. In addition, we also know c_0/c_i based on (4.21), which will be used by frequency domain equalization at the receiver side. According to (4.11) the memoryless nonlinear function can be represented as

$$g(x(n)) \approx \sum_{k=1}^{K} a_k x(n)^k \approx \frac{\sum_{k=1}^{K} b_{k,0} \Psi^k(x(n)) + A_0}{c_0}. \tag{4.24}$$

Although, we do not know the values of $\{a_k\}$ for the memoryless polynomial $g(x(n))$, we can use the polynomial at the right hand side of (4.24) as a replacement for $g(x(n))$. Note that, the value of c_0 is unknown. But it can be absorbed into the polynomial coefficients $\{a_k\}$, so we can simply let $c_0 = 1$. In the final, we obtained a scaled version of the composite ISI channel with the scale factor β_1 and a scaled version of polynomial coefficients with scale factor $\beta_2 = 1/\beta_1$. So, this does not influence their multiplication. It is noted that such scaling operation does not affect the implementation of the receiver.

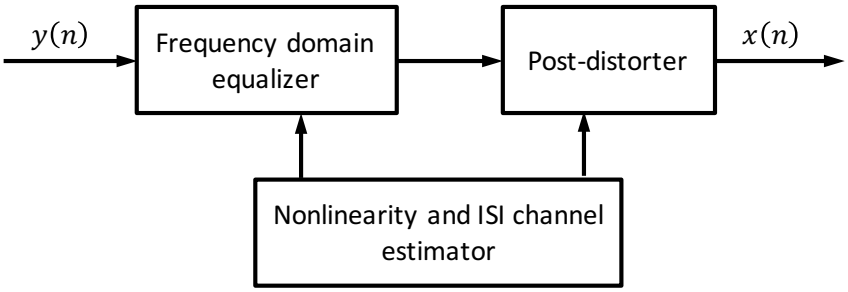

Figure 4.5: Block diagram of receiver structure.

Frequency Domain Equalization and Post Distortion

With the definition of the composite channel vector c and the Hammerstein model for LED, we can rewrite (4.8) as

$$\mathbf{y} = \mathbf{g} * \mathbf{c} + \mathbf{n}, \tag{4.25}$$

where $\mathbf{g}$=$[g(x(M)), g(x(M+1)), \ldots g(x(N)]^T$ given by (4.7). According to (4.9), the system can be regarded as a concatenation of memoryless nonlinear LED and an ISI channel. Hence, besides the nonlinearity and ISI channel estimator, we employ an frequency domain equalizer to combat ISI, followed by a post-distorter to tackle the nonlinear distortion. The structure of the receiver is shown in Fig.4.5. In particular, we propose to use frequency domain equalization due to its low complexity. Assuming that cyclic prefixing is used in the single carrier system, which converts the linear convolution to cyclic convolution, we construct an $(N-M+1)\times(N-M+1)$ circulant composite channel matrix $\mathbf{C}$ with its first column given by $\widetilde{\mathbf{c}} = [\mathbf{c}, \mathbf{0}]^T$, where the length of vector $\mathbf{0}$ is $(N-2M-L+2)$.

The linear convolution model in (4.9) can be rewritten in a matrix form as

$$\mathbf{y} = \mathbf{C}\mathbf{g} + \mathbf{n}. \tag{4.26}$$

Since the circulant matrix $\mathbf{C}$ can be diagonalized by the DFT matrix, i.e., $\mathbf{FCF^H} = \mathbf{D}$,

where $\mathbf{F}$ is the normalized DFT matrix (the $(m,n)th$ element is given by $N^{-1/2}e^{-j2\pi mn/N}$, where $j = \sqrt{-1}$), and the diagonal matrix

$$\mathbf{D} = Diag\{d_M, d_{M+1}, \ldots, d_N\},$$

whose diagonal elements $[d_M, d_{M+1}, \ldots, d_N]^T = \sqrt{N-M+1}\mathbf{F}\widetilde{\mathbf{c}}$. Model (4.26) can be rewritten as

$$\mathbf{Fy} = \mathbf{FCF^H Fg} + \mathbf{Fn}. \tag{4.27}$$

Then we have

$$\mathbf{Fy} = \mathbf{DFg} + \mathbf{Fn}. \tag{4.28}$$

With received signal vector $\mathbf{y}$ and combined channel and memory coefficients $\mathbf{c}$ estimated from the previous part, the LS estimate of the memoryless nonlinear signal $g(x(n))$ can be expressed as

$$\hat{\mathbf{g}} = \mathbf{F^H D^{-1} Fy}. \tag{4.29}$$

The output of the frequency domain equalizer is the input to the post-distorter for nonlinearity mitigation, where the post-distorter is an inverse function of the estimated nonlinear model.

4.3 Simulation Results

In this section, we examine the system performance with the proposed technique in terms of symbol error rate (SER). Also, we compare the mean square error (MSE) of the estimated composite channel and the MSE of the nonlinearity modelling. To account for

the limited LED bandwidth, the LED memory length is 4. The LED nonlinear transfer function is given by the Hammerstein model [128]

$$z(n) = \sum_{k=1}^{K} a_k x(n)^k + \sum_{m=1}^{4} \lambda_m (\sum_{k=1}^{K} a_k x(n-m)^k), \tag{4.30}$$

where to ensure LED acts as a low-pass filter [123], the coefficients $\lambda_1 = 0.3$, $\lambda_2 = 0.25$, $\lambda_3 = 0.2$ and $\lambda_1 = 0.1$, and the polynomial coefficients $\{a_k\}$ are obtained based on a LED data sheet [114]. We choose $K = 4$ and the coefficients are $a_1 = 34.11$, $a_2 = -29.99$, $a_3 = 6.999$, $a_4 = -0.1468$. We consider a room of 5×5×5 m^3 with a single light source on the centre of the celling. Details of the key simulation parameters for the optical wireless channel are summarized in Table 4.1. Based on the channel model in Section 4.2.1, where both LOS component and the first order reflection as the NLOS component of the channel are considered, we can determine the value of the optical wireless channel taps, where we take 5 dominant channel taps and ignore the small ones. It should be noted that higher-order reflection will render a larger channel memory length. But the length of channel memory does not affect the implementation of the proposed scheme. Theoretically, the proposed scheme can deal with any channel memory length. The contribution of this work does not lie on the channel modelling, which has been well investigated. For simplicity, here we only consider first reflection for the NLOS component. The length of training sequence is 100, and 8-PAM with Gray mapping is used.

The LED nonlinearity and the composite optical channel are jointly estimated by the proposed method in Section 4.2.2. Fig.4.6 shows the SER performance of the LED system with various receivers, where the performance of the receiver with perfect knowl-

Table 4.1: Simulation parameters for optical wireless channel.

Parameters	value
Room size	$5 \times 5 \times 5\ m^3$
Reflection coefficient	$\rho = 0.8$
Power	$1\ w$
Lambert's order	1
LED location (x, y, z)	$(2.5, 2.5, 2.15)$
Receiver location (x, y, z)	$(2.5, 2.5, 0)$
Semi-angle at half power	70°
FOV of a receiver	60°
Active area	$1\ cm^2$

edge of composite channel coefficients and LED nonlinearity is also shown for reference. In Fig.4.6, the curve with legend "Ignore LED nonlinearity" denotes the performance of the conventional LS-based linear equalizer where both the LED nonlinearity and memory effect are ignored. It can be seen from the figure that, due to the severe impact of LED nonlinearity and memory effect, the receiver simply does not work. We also show the performance of the recursive LS based post-distortion technique [109] in Fig.4.6, where it is denoted by "conventional RLS post-distortion". It is found that due to the ill-condition of the correlation matrix, the technique doest not work either. In contrast, our proposed technique works very well and its performance is very close to that of the receiver with known LED nonlinearity and composite channel coefficients. In this work, we deal with LED nonlinearity and ISI due to LED memory effect and optical channel jointly. To the best of our knowledge, for the first time, both ISI optical channel and LED nonlinearity with memory effects are jointly estimated and mitigated. The existing works in the literature considered either LED nonlinearity or ISI channel. Accurate joint estimation of LED nonlinearity and composite ISI channel due to the use of orthogonal

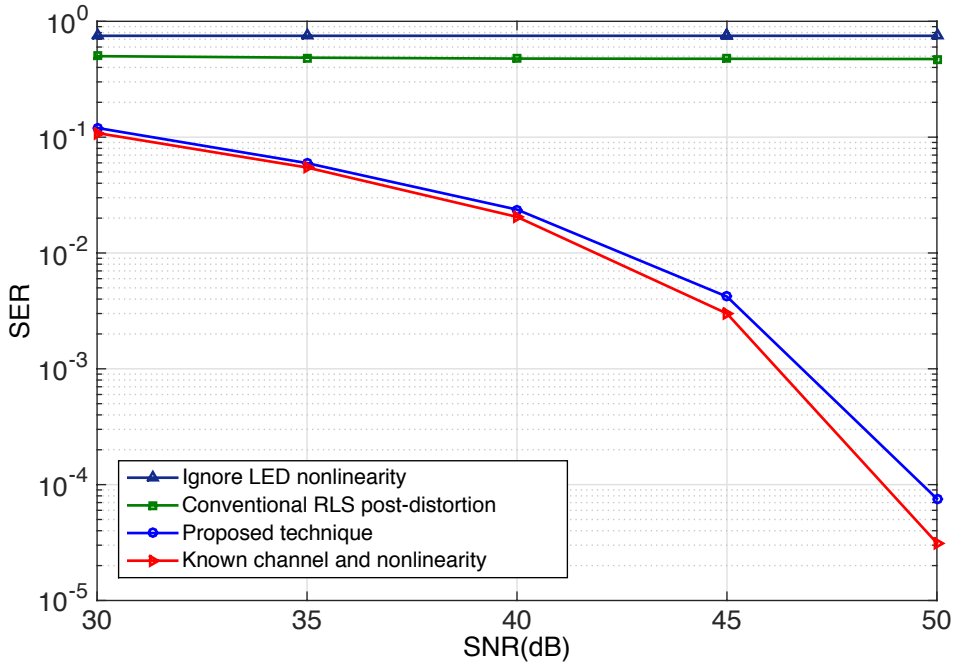

Figure 4.6: SER performance comparison of receivers with 8-PAM and K=4.

polynomials as well as FDE and post-distortion lead to good SER performance. Additionally, we include the mean square error (MSE) of the estimated composite channel as well as the MSE of the nonlinear modelling error as shown in Fig. 4.7 and Fig. 4.8, respectively. The simulation settings are the same as those in Fig.4.6, the results again demonstrate the effectiveness of our proposed technique. In terms of system complexity, the orthogonal polynomial based joint estimation technique circumvents the numerical instability problem in the traditional one and it has low complexity thanks to the quasi-orthogonal property of the basis matrix. Also, the ISI effect is combated through FDE. However, the RLS-based technique has high computational complexity and low convergence rate and sometimes even does not work.

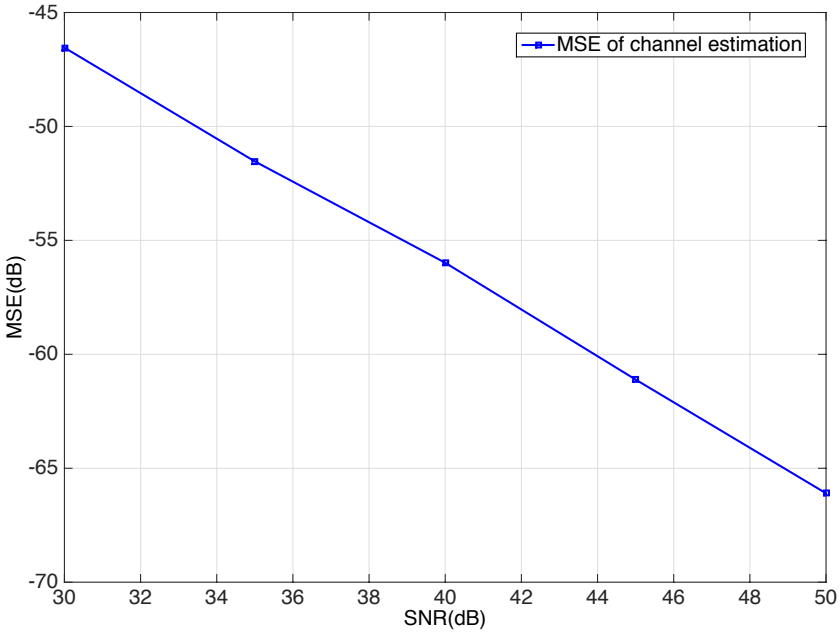

Figure 4.7: MSE of channel estimation.

4.4 Conclusion

In this Chapter, we have investigated joint estimation of LED nonlinearity and optical wireless channel based on the orthogonal polynomial technique. The receiver has been designed, where frequency domain equalization is used to combat ISI, followed by a post-distorter to tackle the LED nonlinearity. The effectiveness of the proposed technique has been verified by simulation results.

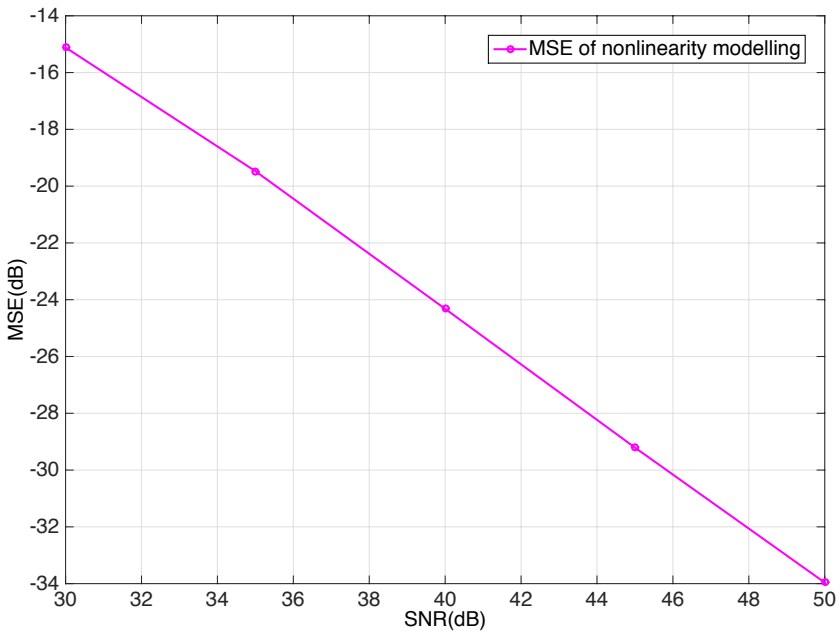

Figure 4.8: MSE of nonlinearity modelling.

Chapter 5

Iterative Nonlinearity Mitigation and Decoding for LED Communications

5.1 Introduction

LED nonlinear distortion may lead to severe performance degradation, various nonlinearity mitigation techniques have been investigated in Chapter 2, which can be categorized into pre-distortion techniques at transmitter side and post-distortion techniques at receiver side. The LED nonlinearity can be modelled as polynomials, and the inverse function of the LED nonlinearity is found directly or indirectly, which is then used by the pre- or post-distorters to compensate the LED nonlinearity [87]. However, as shown in [85], inversion of a nonlinear system cannot be easily achieved and is sometimes only possible for a limited range of input. Also, a nonlinear system of finite order of polynomial cannot be completely compensated by another finite order polynomial [129]. Errors are inevitably generated when deriving the inverse of the nonlinear model. For example,

consider a 3*rd* order memory-less polynomial

$$y = f(x) = a_1 x + a_2 x^2 + a_3 x^3 \tag{5.1}$$

Assume the coefficients $\{a_1, a_2, a_3\}$ are known, and we want to compensate it by another 3*rd* order polynomial, which has the inverse characteristic of the above polynomial

$$z = h(y) = b_1 y + b_2 y^2 + b_3 y^3 \tag{5.2}$$

The output of the above two cascade polynomials is

$$\begin{aligned} z &= b_1(a_1 x + a_2 x^2 + a_3 x^3) + b_2(a_1 x + a_2 x^2 + a_3 x^3)^2 + b_3(a_1 x + a_2 x^2 + a_3 x^3)^3 \\ &= b_1 a_1 x + (b_1 a_2 + b_2 a_1^2) x^2 + (b_1 a_3 + b_3 a_1^3 + 2 b_2 a_1 a_2) x^3 + (3 b_3 a_1^2 a_2 + \\ &\quad 2 b_2 a_1 a_3 + b_2 a_2^2) x^4 + (3 b_3 a_1^2 a_3 + 3 b_3 a_1 a_2^2 + 2 b_2 a_2 a_3) x^5 + (6 b_3 a_1 a_2 a_3 \\ &\quad + b_3 a_2^3 + b_2 a_3^2) x^6 + (3 b_3 a_2^2 a_3 + 3 b_3 a_1 a_3^2) x^7 + 3 b_3 a_2 a_3^2 x^8 + b_3 a_3^3 x^9 \end{aligned} \tag{5.3}$$

As we only have 3 control variables, we can only mitigate up to 3*rd* order nonlinear distortions with the following requirements

$$b_1 a_1 = G \tag{5.4}$$

$$b_1 a_2 + b_2 a_1^2 = 0 \tag{5.5}$$

$$(b_1 a_3 + b_3 a_1^3 + 2 b_2 a_1 a_2) = 0 \tag{5.6}$$

where G is the linear gain. We can see that a *pth* order polynomial can only mitigate up to *pth* order nonlinear distortions. The residual nonlinear distortions with order higher than p are inevitably generated. Pre-distortion ahead of the nonlinear device is an effective method for compensating the nonlinear distortions. However, pre-distortion techniques are not cost-efficient as it needs feedback path from the receiver to transmitter. Additional physical modules and circuits are needed, which increases the system complexity and power efficiency. As post-distortion is implemented at receiver side, it is more convenient to use and adaptive distortion can be easily realised to handle the time-varying nonlinearity of LEDs. Hence, in this Chapter we focus on post-distortion. In [109], the author proposed an adaptive post-distortion technique. It has the advantage in terms of system complexity over pre-distortion methods. However, another problem of conventional post-distortion technique is that noise is added at the receiver side. The inverse nonlinear operation to the received signal will cause colour noises, which affects the overall system performance.

In this Chapter, we consider iterative nonlinearity mitigation and decoding in a coded LED communication system and design an iterative receiver, which consists of a soft-in-soft-out (SISO) post-distorter and a SISO decoder. The SISO post-distorter and the decoder work in an iterative manner by exchanging the log-likelihood ratios (LLRs) of coded bits. Specifically, the SISO post-distorter computes the extrinsic LLRs of coded bits based on the feedback from the SISO decoder, the observations at the receiver side and the nonlinearity of the LED. The polynomial inversion is not needed in the proposed technique (which is different from the conventional techniques), therefore avoiding the errors due to the use of finite-order inverse polynomials and the generation of colour noises. To the best of our knowledge, iterative nonlinearity mitigation technique has

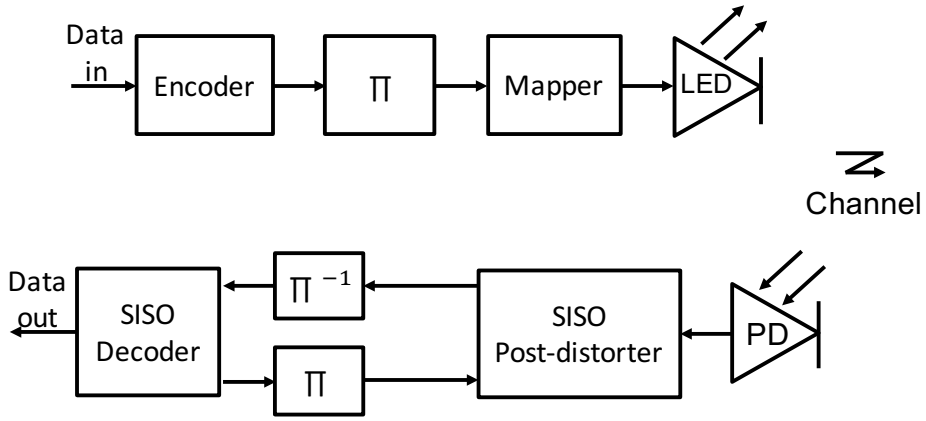

Figure 5.1: Block diagram of iterative nonlinearity mitigation and decoding, where Π and Π^{-1} denote an interleaver and the corresponding deinterleaver, respectively.

not been investigated before. It is demonstrated that a remarkable performance gain can be achieved by the interaction between the SISO post-distorter and the SISO decoder through the iterative process. In addition, the iterative receiver converges very fast, as shown by the examples in the simulation results.

The organization of this Chapter is as follows. In Section 5.2, the signal model is introduced, and then the receiver design for iterative LED nonlinearity mitigation and decoding is investigated in detail. Simulation results are provided in Section 5.3 to verify the effectiveness of our proposed method. The Chapter is concluded in Section 5.4.

5.2 Iterative SISO Detector

5.2.1 Signal Model

We assume a single-carrier coded LED communication system with PAM modulation. As shown in the upper part of Fig. 5.1, at the transmitter side, information bits are firstly encoded into a code sequence and passed through an interleaver. The interleaved code sequence $\boldsymbol{c}$ is then divided into length-L sub-sequences $[c_{n,1}, c_{n,2}, \ldots, c_{n,L}]$ and each sub-

sequence is mapped to a 2^L-ary PAM symbol $x(n) \in \beta = \{\alpha_i, i = 1, 2, \ldots, 2^L\}$ with a mapping rule (e.g., Gray mapping). Symbols $\{x_n\}$ are then used to modulate the LED light intensity for transmission. Due to the nonlinearity of the LED, the transmitted signal can be represented as [60]

$$z_n = \sum_{k=1}^{K} \sum_{m=0}^{M} a_{k,m} x_{n-m}^k, \tag{5.7}$$

where the nonlinearity of the LED is modelled as a Kth order memory polynomial with coefficients $\{a_{k,m}\}$ and M is the memory length. It should be noted that the inter-symbol interference (ISI) channel due to multipath propagation can be absorbed into the memory polynomial model in (5.7). The signal is picked up by the photo diode (PD) and converted to an electrical one, which can be represented as

$$y_n = \rho z_n + w_n, \tag{5.8}$$

where ρ is the PD responsivity that is set to unity for simplicity, and w_n denotes the additive white Gaussian noise (AWGN) with power σ^2.

The focus of this work is the receiver design and an iterative LED nonlinearity mitigation and decoding technique is proposed. We assume that the memory polynomial coefficients are known, and they can be estimated with the techniques e.g., our proposed orthogonal polynomial technique in Chapter 3 [118], and [57], etc.

5.2.2 Receiver Design for Iterative LED Nonlinearity Mitigation and Decoding

The iterative receiver is shown in the lower part of Fig. 5.1. It contains a SISO post-distorter and a SISO decoder, which work in an iterative manner by exchanging the extrinsic LLRs of coded bits.

Specifically, the SISO post-distorter computes the extrinsic LLRs for each coded bit with the output extrinsic LLRs from the decoder as the *a priori* information, and with the extrinsic LLRs from the post-distorter, the decoder refines the LLRs with the code constraints.

In this work, we borrow the standard SISO decoding algorithms (e.g., the BCJR algorithm for the convolutional codes) for the decoder, and focus on the derivation of the SISO post-distorter.

The task of the post-distorter is to compute the LLR for each code bit $c_{n,l}$ (without taking coding into account), which can be expressed as

$$\begin{aligned} LLR^p(c_{n,l}) &= ln\frac{p(c_{n,l}=0|\mathbf{y})}{p(c_{n,l}=1|\mathbf{y})} \\ &= ln\frac{\sum_{\alpha_i\in\beta_l^0} p(x_n=\alpha_i|\mathbf{y})}{\sum_{\alpha_i\in\beta_l^1} p(x_n=\alpha_i|\mathbf{y})}, \end{aligned} \tag{5.9}$$

where β_l^0 and β_l^1 denote the subsets of all $\alpha_i \in \beta$ whose label in position l has the value of 0 and 1, respectively, and $\mathbf{y} = [y_1, y_2, \dots]$ is the received signal vector.

For the iterative receiver shown in Fig.5.1, the extrinsic LLR should be used accord-

ing to the turbo principle. The extrinsic LLR

$$LLR^e(c_{n,l}) = LLR^p(c_{n,l}) - LLR^a(c_{n,l}), \tag{5.10}$$

will be input to the decoder, where $LLR^a(c_{n,l})$ is the *a priori* LLR from the decoder in the previous iteration.

From the above, it can be seen that the key is to compute the *a posteriori* probability of each transmitted symbol $p(x_n|\mathbf{y})$. According to Bayes' theorem [130], we have

$$p(x_n|\mathbf{y}) = \frac{p(\mathbf{y}|x_n)p(x_n)}{p(\mathbf{y})}, \tag{5.11}$$

where $p(x_n)$ is the *a priori* probability of the symbol x_n and $p(\mathbf{y})$ is a constant for a fixed received signal. Then, we have

$$p(x_n|\mathbf{y}) \propto p(\mathbf{y}|x_n)p(x_n), \tag{5.12}$$

$p(x_n)$ can be calculated based on the feedback from the decoder, i.e., Firstly with the *a priori* LLR

$$LLR^a(c_{n,l}) = ln\frac{p(c_{n,l} = 0)}{p(c_{n,l} = 1)}, \tag{5.13}$$

fed back from the decoder and

$$p(c_{n,l} = 0) + p(c_{n,l} = 1) = 1. \tag{5.14}$$

We convert the *a priori* LLR to bit probability as

$$p(c_{n,l} = 0) = \frac{1}{1 + exp(LLR^a(c_{n,l}))}, \tag{5.15}$$

$$p(c_{n,l} = 1) = 1 - p(c_{n,l} = 0). \tag{5.16}$$

The probability of the transmitted symbols $p(x_n = \alpha_i)$ can be calculated as

$$p(x_n = \alpha_i) = \prod_{j=1}^{M} p(c_{n,j} = s_{i,j}), \tag{5.17}$$

where each α_i corresponds to a binary vector $\mathbf{s}_i = [s_{i,1}, s_{i,2}, \ldots, s_{i,L}]$. Next, we compute the likelihood $p(\mathbf{y}|x_n)$ for each x_n.

We use a sliding window approach to approximately compute the likelihood in (5.12). Define $\mathbf{y_n} = [y_n, \ldots, y_{n+M}]^T$ and $\mathbf{w_n} = [w_n, \ldots, w_{n+M}]^T$, and we compute $p(\mathbf{y_n}|x_n)$ instead of $p(\mathbf{y}|x_n)$. Based on (7) and (8), we have

$$\mathbf{y_n} = \underbrace{\begin{bmatrix} \sum_{k=1}^{K} a_{k,0} x_n^k \\ \vdots \\ \sum_{k=1}^{K} a_{k,M} x_n^k \end{bmatrix}}_{\mathbf{a}(x_n)} + \underbrace{\begin{bmatrix} \sum_{k=1}^{K} \sum_{m=1}^{M} a_{k,m} x_{n-m}^k \\ \vdots \\ \sum_{k=1}^{K} \sum_{m=0}^{M-1} a_{k,m} x_{n+M-m}^k \end{bmatrix}}_{\mathbf{i}} + \mathbf{w_n}, \tag{5.18}$$

where $\mathbf{a}(x_n)$ is the useful signal related to x_n, and $\mathbf{i}$ is the interference.

We approximate the interference $\mathbf{i}$ to be Gaussian and its mean $\mathbf{i}'$ and covariance matrix $\mathbf{R}$ can be easily calculated based on the feedback of the decoder. Then we have

$$p(\mathbf{y_n}|x_n = \alpha_i) \propto \exp(-\frac{1}{2}[\mathbf{y_n} - \mathbf{a}(\alpha_i) - \mathbf{i}']^T \mathbf{V}^{-1} [\mathbf{y_n} - \mathbf{a}(\alpha_i) - \mathbf{i}']), \tag{5.19}$$

where $\mathbf{V} = \mathbf{R} + \sigma^2\mathbf{I}$. To reduce the complexity, we ignore the correlation between the elements in $\mathbf{i}$, so that $\mathbf{R}$ is approximated as a diagonal matrix. Hence, the matrix inversion $\mathbf{V}^{-1}$ is trivial and the evaluation of (5.19) actually only involves scalar operations, thus leading to low complexity. Then, we normalize $p(x_n = \alpha_i|\mathbf{y_n})$ as

$$p(x_n = \alpha_i|\mathbf{y_n}) = \frac{p(x_n = \alpha_i|\mathbf{y_n})}{\sum_{i=1}^{2^L} p(x_n = \alpha_i|\mathbf{y_n})}. \tag{5.20}$$

The operations involved in our proposed iterative nonlinearity and decoding technique are summarized as follows:

- Step 1: with nonlinear parameters, perform likelihood estimation to find the *a posteriori* symbol probability $p(x_n = \alpha_i|\mathbf{y_n})$
- Step2: convert the symbol level probability $p(x_n = \alpha_i|\mathbf{y_n})$ to bit level probability $LLR^p(c_{n,l})$ for each coded bit
- Step3: calculate the extrinsic *a priori* LLR $LLR^a(c_{n,l})$ for each coded bit
- Step4: calculate the *a priori* symbol probability $p(x_n = \alpha_i)$ for next iteration

It can be seen from the above that, no polynomial inversion is required in the proposed technique, therefore avoiding the errors due to the use of finite-order inverse polynomials and the generation of colour noises.

5.3 Simulation results

In the simulations, 8-PAM is used for modulation and the convolutional code with generator [171,133] is used for generating codewords with length 1200. We compare the

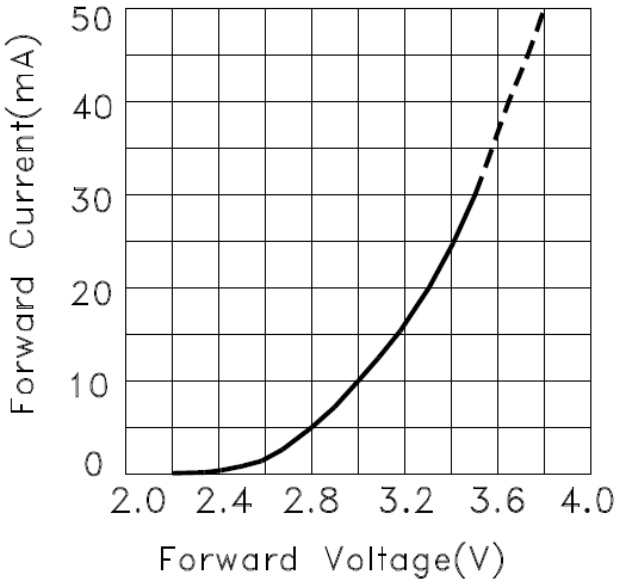

Figure 5.2: Kingbright blue T-1 3/4 (5mm) LED V-I datasheet [114].

system BER performance of our proposed iterative nonlinearity mitigation and decoding technique with conventional non-iterative and iterative post-distortion techniques. The LED nonlinear transfer function is given by the Hammerstein model [128]

$$z_n = \sum_{k=1}^{K} a_k x_n^k + \lambda(\sum_{k=1}^{K} a_k x_{n-1}^k), \tag{5.21}$$

where $\lambda = 0.1$. The polynomial coefficients $\{a_k\}$ are obtained based on an LED datasheet (Kingbright blue T-1 3/4 (5mm) LED)[114], which is shown in Fig. 5.2 for convenience. We choose $K = 4$ and the coefficients $a_1 = 34.11$, $a_2 = -29.99$, $a_3 = 6.999$ and $a_4 = -0.1468$.

Fig. 5.3 shows the BER performance of the various receivers. The non-iterative receiver employs the frequency domain equalization (FDE) to compensate the memory effect [121] and the conventional polynomial inverse technique [131] as post-distortion, followed by hard Viterbi decoding. Iterative receiver a represents the conventional iterative equalization and decoding receiver where the nonlinearity of the LED is simply

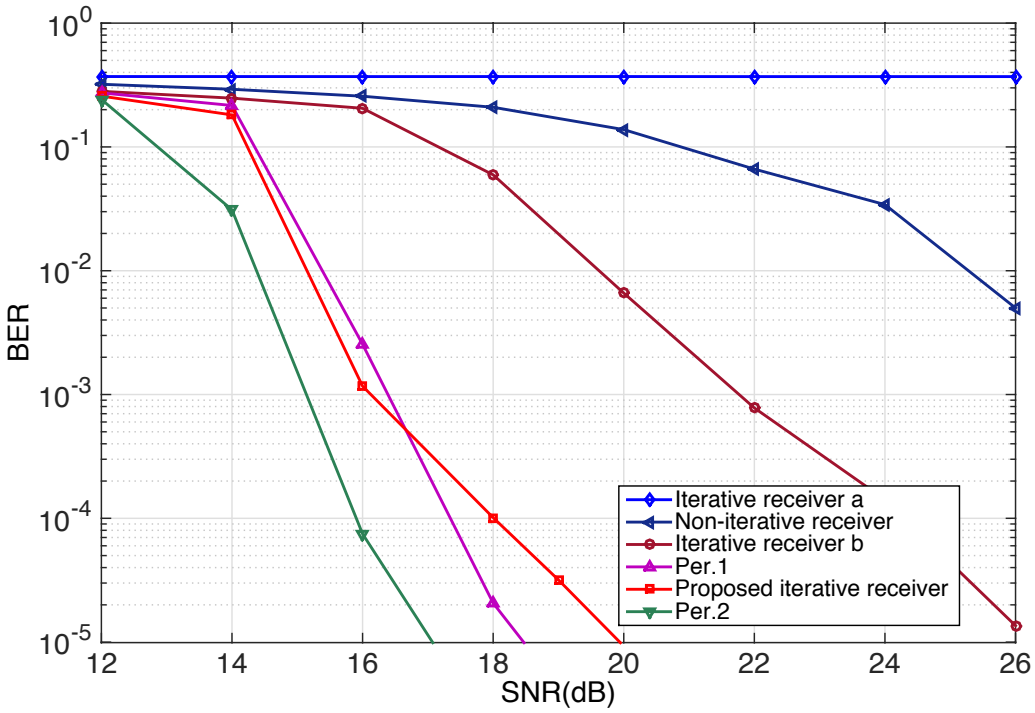

Figure 5.3: Comparison of system BER performance.

ignored. It can be seen that, due to the lack of the nonlinearity mitigation mechanism, Iterative receiver a does not work properly. Iterative receiver b employs the same FDE and polynomial inverse technique as the non-iterative receiver (to combat the LED memory effect and nonlinearity) followed by the conventional iterative demapping and decoding technique. It can be seen that, thanks to the iterative demapping and decoding, Iterative receiver b delivers much better performance than the non-iterative receiver, but it is significantly inferior to the proposed iterative receiver (where iterative nonlinearity mitigation is used). The performances of the system without nonlinearity and memory are also shown for reference, where we assume an ideal LED with linear transfer function, and they are denoted by "Per. 1" and "Per. 2" in Fig. 5.3. In Per. 1, the signal power at the output of the ideal LED (which has the same turn-on voltage as the non-ideal one) is the same as that of the non-ideal LED. In Per. 2, the dynamic range of the ideal LED is

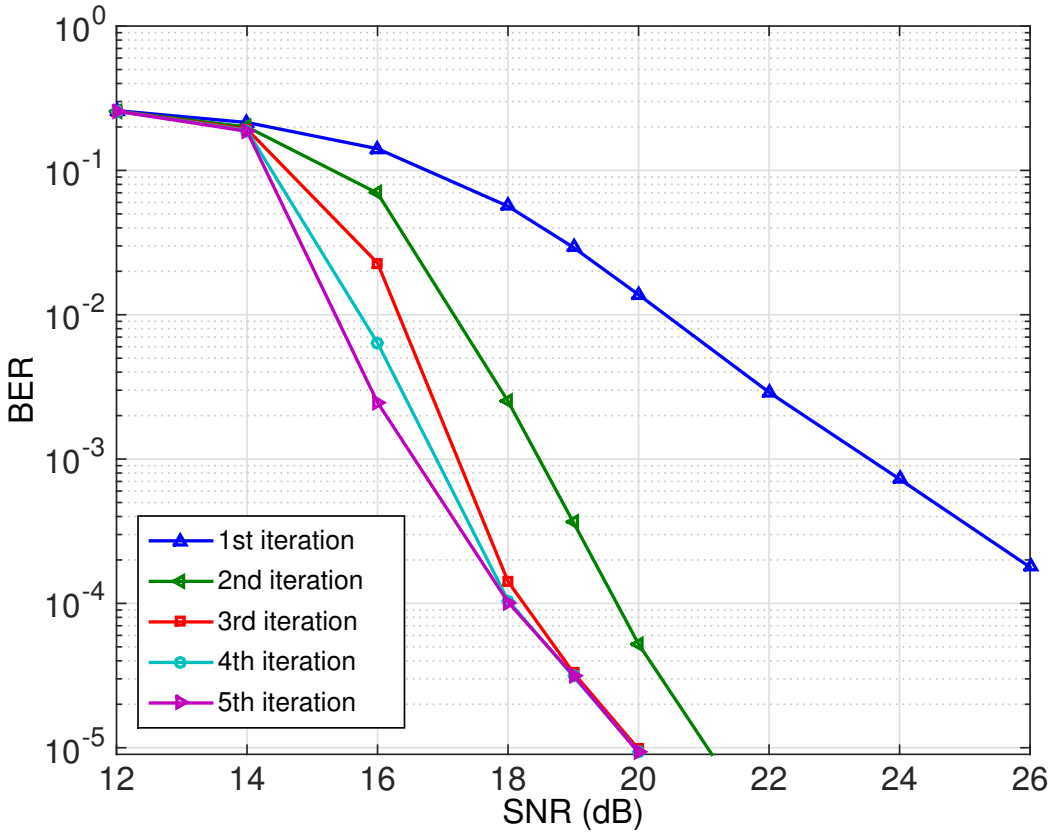

Figure 5.4: Performance of the proposed iterative receiver with different iterations.

the same as that of the non-ideal one. It can be seen from Fig. 5.3 that, the performance of our receiver has a small gap with Per. 2 because the signal power at the output of the ideal LED is larger than that of the non-ideal LED. We can also see that the performance of our receiver is very close to Per. 1, which demonstrates the effectiveness of the proposed nonlinearity mitigation technique. Fig. 5.4 shows the performance of the proposed iterative receiver with different iterations, where we can see that the iterative receiver converges fast and it only requires 3-5 iterations.

5.4 Conclusion

In this Chapter, we have proposed an iterative post-distortion technique to mitigate the nonlinear distortion in LED communications. A SISO post-distorter has been designed, which works iteratively with the SISO decoder in the system. It has been demonstrated that a remarkable performance gain can be achieved by the iterative receiver compared with conventional iterative and non-iterative post-distortion techniques.

Chapter 6

Conclusions and Future Work

6.1 Conclusions

In this thesis, we have investigated and proposed some efficient and effective nonlinear system modelling and mitigation techniques in LED communications. The memory effect of LED and ISI distortions are also solved. The major contributions of this thesis are summarized in the following.

In Chapter 2, we do an overall literature review of the current work on LED communications. Firstly, the IM/DD system for LED communications and various modulation techniques specially designed for LED communications are introduced. Then, we focus on the LED nonlinear problem and introduce some popular nonlinear models being used for system modelling. Lastly, we investigate some current works on nonlinear system modelling and nonlinearity mitigation techniques. The problems of the existing works are our concerns and we aim to solve these in our research.

In Chapter 3, to solve the numerical instability problem in finding the memory polynomial coefficients in the conventional LED nonlinearity modelling techniques, we pro-

posed an alternative LED nonlinearity modelling technique based on orthogonal polynomials. For the first time, we developed a special set of orthogonal polynomial basis for LED communications with PAM signalling to achieve effective and efficient LED nonlinear system modelling. Due to the use of the orthogonal polynomials, the new basis matrix for the nonlinear model is a quasi-orthogonal matrix, avoiding the numerical instability problem during the estimation of the polynomial coefficients, which leads to low complexity and accurate LED nonlinearity modelling. Furthermore, a pre-distorter is employed to mitigate the LED nonlinearity. Simulations show that, compared to the conventional memory polynomial based technique, our technique significantly outperforms the conventional technique in terms of LED nonlinearity modelling error and system SER performance.

In Chapter 4, we extend our previous work on orthogonal polynomial based LED modelling technique and consider both the LED nonlinearity and ISI distortions due to LED memory effect and multipath dispersion in indoor LED communications. We develop a joint estimation approach to LED nonlinearity and composite ISI channel due to the LED memory effect and optical wireless channel based on our orthogonal polynomial technique. The orthogonal polynomial based joint estimation technique circumvents the numerical instability problem over the traditional one and it has low complexity thanks to the orthogonal property of the basis matrix. Then, we design a receiver which consists of three modules including nonlinearity and composite channel estimator, FDE equalizer and nonlinearity mitigator. In this work, we deal with LED nonlinearity and ISI due to LED memory effect and optical channel jointly. To the best of our knowledge, for the first time, both ISI optical channel and LED nonlinearity with memory effects are jointly estimated and mitigated. Simulations show that the proposed technique can effectively

handle the LED nonlinearity and ISI distortion.

In Chapter 5, with effective LED nonlinearity modelling technique developed, we consider iterative nonlinearity mitigation and decoding in a coded LED communication system and design an iterative receiver, which consists of a SISO post-distorter and a SISO decoder. To the best of knowledge, for the first time, the post distorter is combined with demapper to handle the distortion of LED nonlinearity and ISI (due to LED and channel), and a SISO post-distorter is developed. The SISO post-distorter and the decoder work in an iterative manner by exchanging the LLRs of coded bits. Specifically, the SISO post-distorter iteratively finds the *a posteriori* probability estimates of the data symbols based on the nonlinearity parameter and *a priori* information from the SISO decoder. It is very different from the conventional post-distorters as explicit polynomial inversion is not required, thereby avoiding the impact of imperfect polynomial inversion and the generation of colour noises. Simulations show that the proposed scheme allows iterative interaction with the decoder, leading to remarkable performance gain, compared to the conventional one. In addition, the iterative receiver converges very fast which is effective and efficient.

6.2 Future Work

The thesis has successfully developed an effective and efficient nonlinear system and ISI channel modelling technique based on orthogonal polynomial for LED communications. A joint LED nonlinearity and composite ISI channel estimation and mitigation technique has been proposed. A novel iterative nonlinearity mitigation and decoding technique with SISO post-distorter and SISO decoder has been designed to significantly improve

the performance of post-distortion. However, there are still some issues that need to be further studied.

- Develop iterative post-distortion with precoding

  The nature drawback of post-distortion technique is that noise is added at the receiver side. Signals within the most severe nonlinear region will be affected more significantly, which may dominant the overall system performance. We believe with appropriate precoding technique at the transmitter side and iterative demapping and decoding post-distortion at the receiver side. The iterative receiver combined with the correlation between the transmitted information bits will helpful to further improve the system performance of post-distortion.

- Post-distortion with approximate linearization

  The conventional post-distortion or pre-distortion techniques require finding the inverse of the nonlinear function, which will inevitably has residual error. We have proposed a iterative SISO post-distorter and demapper associated with SISO decoder to solve this issue in Chapter 5. We believe post-distortion with approximate linearization using Taylor expansion may be another alternative. With estimated nonlinear function, we can do Taylor expansion at a specific point and ignore the higher order items to achieve a approximate linear function.

Bibliography

(1) G. Pang, “Information technology based on visible LEDs for optical wireless communications”, *TENCON 2004. 2004 IEEE Region 10 Conference*, 2004, 395–398.

(2) G. Pang, T. Kwan, H. Liu and C.-H. Chan, “LED wireless”, *IEEE Industry Applications Magazine*, 2002, **8**, 21–28.

(3) H. Le Minh, D. O’Brien, G. Faulkner, L. Zeng, K. Lee, D. Jung, Y. Oh and E. T. Won, “100-Mb/s NRZ visible light communications using a postequalized white LED”, *IEEE Photonics Technology Letters*, 2009, **21**, 1063–1065.

(4) K.-D. Langer, J. Vučić, C. Kottke, L. Fernández, K. Habe, A. Paraskevopoulos, M. Wendl and V. Markov, “Exploring the potentials of optical-wireless communication using white LEDs”, *Transparent Optical Networks (ICTON), 2011 13th International Conference on*, 2011, 1–5.

(5) W. Rui, D. Jing-Yuan, S. An-Cun, W. Yong-Jie and L. Yu-Liang, “Indoor optical wireless communication system utilizing white LED lights”, *Communications, 2009. APCC 2009. 15th Asia-Pacific Conference on*, 2009, 617–621.

(6) S.-Y. Jung, S. Hann and C.-S. Park, "TDOA-based optical wireless indoor localization using LED ceiling lamps", *IEEE Transactions on Consumer Electronics*, 2011, **57**.

(7) J. Armstrong, Y. Sekercioglu and A. Neild, "Visible light positioning: a roadmap for international standardization", *IEEE Communications Magazine*, 2013, **51**, 68–73.

(8) M. Yoshino, S. Haruyama and M. Nakagawa, "High-accuracy positioning system using visible LED lights and image sensor", *Radio and Wireless Symposium, 2008 IEEE*, 2008, 439–442.

(9) P. Tian, X. Liu, S. Yi, Y. Huang, S. Zhang, X. Zhou, L. Hu, L. Zheng and R. Liu, "High-speed underwater optical wireless communication using a blue GaN-based micro-LED", *Optics express*, 2017, **25**, 1193–1201.

(10) J. Rao, W. Wei, F. Wang and X. Zhang, "An underwater optical wireless communication system based on LED source", *Photonics and Optoelectronics Meetings (POEM) 2011: Optical Communication Systems and Networking*, 2012, **8331**, 83310N.

(11) Z. Zeng, S. Fu, H. Zhang, Y. Dong and J. Cheng, "A survey of underwater optical wireless communications", *IEEE Communications Surveys & Tutorials*, 2017, **19**, 204–238.

(12) H. Kaushal and G. Kaddoum, "Underwater optical wireless communication", *IEEE Access*, 2016, **4**, 1518–1547.

(13) J.-H. Yoo, J.-S. Jang, J. Kwon, H.-C. Kim, D.-W. Song and S.-Y. Jung, "Demonstration of vehicular visible light communication based on LED headlamp", *International journal of automotive technology*, 2016, **17**, 347–352.

(14) A.-M. Cailean, B. Cagneau, L. Chassagne, V. Popa and M. Dimian, "A survey on the usage of DSRC and VLC in communication-based vehicle safety applications", *Communications and Vehicular Technology in the Benelux (SCVT), 2014 IEEE 21st Symposium on*, 2014, 69–74.

(15) N. Kumar, N. Lourenço, D. Terra, L. N. Alves and R. L. Aguiar, "Visible light communications in intelligent transportation systems", *Intelligent Vehicles Symposium (IV), 2012 IEEE*, 2012, 748–753.

(16) Y. Tanaka, S. Haruyama and M. Nakagawa, "Wireless optical transmissions with white colored LED for wireless home links", *Personal, Indoor and Mobile Radio Communications, 2000. PIMRC 2000. The 11th IEEE International Symposium on*, 2000, **2**, 1325–1329.

(17) Y. Tanaka, T. Komine, S. Haruyama and M. Nakagawa, "Indoor visible light data transmission system utilizing white LED lights", *IEICE transactions on communications*, 2003, **86**, 2440–2454.

(18) T. Komine and M. Nakagawa, "Fundamental analysis for visible-light communication system using LED lights", *IEEE transactions on Consumer Electronics*, 2004, **50**, 100–107.

(19) T. Komine and M. Nakagawa, "Integrated system of white LED visible-light communication and power-line communication", *IEEE Transactions on Consumer Electronics*, 2003, **49**, 71–79.

(20) J.-P. Javaudin, M. Bellec, D. Varoutas and V. Suraci, "OMEGA ICT project: Towards convergent Gigabit home networks", *Personal, Indoor and Mobile Radio Communications, 2008. PIMRC 2008. IEEE 19th International Symposium on*, 2008, 1–5.

(21) D. C. O'Brien, G. Faulkner, H. Le Minh, O. Bouchet, M. El Tabach, M. Wolf, J. W. Walewski, S. Randel, S. Nerreter, M. Franke et al., "Home access networks using optical wireless transmission", *Personal, Indoor and Mobile Radio Communications, 2008. PIMRC 2008. IEEE 19th International Symposium on*, 2008, 1–5.

(22) K.-D. Langer, J. Grubor, O. Bouchet, M. El Tabach, J. W. Walewski, S. Randel, M. Franke, S. Nerreter, D. C. O'Brien, G. E. Faulkner et al., "Optical wireless communications for broadband access in home area networks", *Transparent Optical Networks, 2008. ICTon 2008. 10th Anniversary International Conference on*, 2008, **4**, 149–154.

(23) D. Tsonev, S. Videv and H. Haas, "Light fidelity (Li-Fi): towards all-optical networking", *Broadband Access Communication Technologies VIII*, 2014, **9007**, 900702.

(24) G. Kant, V. Gogate and V. Kotak, "Li-Fi Need of 21 st Century", 2017.

(25) H. Haas, L. Yin, Y. Wang and C. Chen, "What is lifi?", *Journal of Lightwave Technology*, 2016, **34**, 1533–1544.

(26) R. J. Green, H. Joshi, M. D. Higgins and M. S. Leeson, "Recent developments in indoor optical wireless systems", *IET communications*, 2008, **2**, 3–10.

(27) "http://www.bemri.org/visible-light-communication/documents-and-present atio ns/422-visible-light-communications-achieving-high-data-rates/file.html".

(28) Y. Wang, X. Huang, L. Tao, J. Shi and N. Chi, "4.5-Gb/s RGB-LED based WDM visible light communication system employing CAP modulation and RLS based adaptive equalization", *Optics express*, 2015, **23**, 13626–13633.

(29) H.-H. Chou, S.-K. Liaw, C. Teng, J.-S. Jiang, C.-Y. Tsai, C.-J. Wu and M.-J. Chien, "RGB LEDs visible light communications based on equalized receiver with broadband optical filters", *Fiber Optics in Access Network (FOAN), 2015 International Workshop on*, 2015, 22–25.

(30) Y. Wang, Y. Wang, N. Chi, J. Yu and H. Shang, "Demonstration of 575-Mb/s downlink and 225-Mb/s uplink bi-directional SCM-WDM visible light communication using RGB LED and phosphor-based LED", *Optics express*, 2013, **21**, 1203–1208.

(31) D. C. O'Brien, L. Zeng, H. Le-Minh, G. Faulkner, J. W. Walewski and S. Randel, "Visible light communications: Challenges and possibilities", *Personal, Indoor and Mobile Radio Communications, 2008. PIMRC 2008. IEEE 19th International Symposium on*, 2008, 1–5.

(32) J. Grubor, K. Langer, J. Walewski and S. Randel, "High-speed wireless indoor communication via visible light", *ITG fachbericht*, 2007, **198**, 203.

(33) T. Fath, C. Heller and H. Haas, "Optical wireless transmitter employing discrete power level stepping", *Journal of Lightwave Technology*, 2013, **31**, 1734–1743.

(34) J. Vučić, C. Kottke, S. Nerreter, K. Habel, A. Büttner, K.-D. Langer and J. W. Walewski, "230 Mbit/s via a wireless visible-light link based on OOK modula-

tion of phosphorescent white LEDs", *Optical Fiber Communication Conference*, 2010, OThH3.

(35) D. J. Barros, S. K. Wilson and J. M. Kahn, "Comparison of orthogonal frequency-division multiplexing and pulse-amplitude modulation in indoor optical wireless links", *IEEE Transactions on Communications*, 2012, **60**, 153–163.

(36) S. D. Dissanayake and J. Armstrong, "Comparison of aco-ofdm, dco-ofdm and ado-ofdm in im/dd systems", *Journal of lightwave technology*, 2013, **31**, 1063–1072.

(37) S. Dimitrov, S. Sinanovic and H. Haas, "Signal shaping and modulation for optical wireless communication", *Journal of lightwave technology*, 2012, **30**, 1319–1328.

(38) H. Elgala, R. Mesleh and H. Haas, "Practical considerations for indoor wireless optical system implementation using OFDM", *Telecommunications, 2009. ConTEL 2009. 10th International Conference on*, 2009, 25–29.

(39) J. Armstrong and B. J. Schmidt, "Comparison of asymmetrically clipped optical OFDM and DC-biased optical OFDM in AWGN", *IEEE Communications Letters*, 2008, **12**.

(40) J. Armstrong, "OFDM for optical communications", *Journal of lightwave technology*, 2009, **27**, 189–204.

(41) J. Armstrong and A. Lowery, "Power efficient optical OFDM", *Electronics letters*, 2006, **42**, 370–372.

(42) M. F. Sanya, C. Aupetit-Berthelemot, L. Djogbe and A. Vianou, "DC ACO-OFDM and DCO-OFDM for passive optical network: Performance comparison in IM/DD fiber link", *Wireless and Optical Communication Conference (WOCC), 2014 23rd*, 2014, 1–5.

(43) K. Asadzadeh, A. Dabbo and S. Hranilovic, "Receiver design for asymmetrically clipped optical OFDM", *GLOBECOM Workshops (GC Wkshps), 2011 IEEE*, 2011, 777–781.

(44) S. Lee, F. Breyer, D. Cardenas, S. Randel and A. Koonen, "Real-time gigabit DMT transmission over plastic optical fibre", *Electronics letters*, 2009, **45**, 1342–1343.

(45) N. Chi, Y. Wang, Y. Wang, X. Huang and X. Lu, "Ultra-high-speed single red-green-blue light-emitting diode-based visible light communication system utilizing advanced modulation formats", *Chinese Optics Letters*, 2014, **12**, 010605.

(46) Z. Wang, Q. Wang, S. Chen and L. Hanzo, "An adaptive scaling and biasing scheme for OFDM-based visible light communication systems", *Optics express*, 2014, **22**, 12707–12715.

(47) K. Asatani and T. Kimura, "Analyses of LED nonlinear distortions", *IEEE Transactions on Electron Devices*, 1978, **25**, 199–207.

(48) N. Theofanous and A. Arapoyianni, "Light-to-input nonlinearities in an R-LED series network", *IEEE journal of quantum electronics*, 1992, **28**, 34–38.

(49) H. Elgala, R. Mesleh and H. Haas, "A study of LED nonlinearity effects on optical wireless transmission using OFDM", *Wireless and Optical Communications Networks, 2009. WOCN'09. IFIP International Conference on*, 2009, 1–5.

(50) H. Elgala, R. Mesleh and H. Haas, "An LED model for intensity-modulated optical communication systems", *IEEE Photonics Technology Letters*, 2010, **22**, 835–837.

(51) H. Elgala, R. Mesleh and H. Haas, "Impact of LED nonlinearities on optical wireless OFDM systems", *Personal Indoor and Mobile Radio Communications (PIMRC), 2010 IEEE 21st International Symposium on*, 2010, 634–638.

(52) F. Pancaldi, G. M. Vitetta, R. Kalbasi, N. Al-Dhahir, M. Uysal and H. Mheidat, "Single-carrier frequency domain equalization", *IEEE Signal Processing Magazine*, 2008, **25**.

(53) S. Dimitrov, S. Sinanovic and H. Haas, "Clipping noise in OFDM-based optical wireless communication systems", *IEEE Transactions on Communications*, 2012, **60**, 1072–1081.

(54) D. Falconer, S. L. Ariyavisitakul, A. Benyamin-Seeyar and B. Eidson, "Frequency domain equalization for single-carrier broadband wireless systems", *IEEE Communications Magazine*, 2002, **40**, 58–66.

(55) N. Al-Dhahir, "Single-carrier frequency-domain equalization for space-time block-coded transmissions over frequency-selective fading channels", *IEEE Communications Letters*, 2001, **5**, 304–306.

(56) H. Qian, J. Chen, S. Yao, Z. Y. Zhang, H. Zhang and W. Xu, "One-bit sigma-delta modulator for nonlinear visible light communication systems", *IEEE Photonics Technology Letters*, 2015, **27**, 419–422.

(57) D. R. Morgan, Z. Ma, J. Kim, M. G. Zierdt and J. Pastalan, "A generalized memory polynomial model for digital predistortion of RF power amplifiers", *IEEE Transactions on signal processing*, 2006, **54**, 3852–3860.

(58) T. Jiang and G. Zhu, "Nonlinear companding transform for reducing peak-to-average power ratio of OFDM signals", *IEEE Transactions on Broadcasting*, 2004, **50**, 342–346.

(59) T. Jiang, Y. Yang and Y.-H. Song, "Exponential companding technique for PAPR reduction in OFDM systems", *IEEE Transactions on broadcasting*, 2005, **51**, 244–248.

(60) K. Ying, Z. Yu, R. J. Baxley, H. Qian, G.-K. Chang and G. T. Zhou, "Nonlinear distortion mitigation in visible light communications", *IEEE Wireless Communications*, 2015, **22**, 36–45.

(61) E. F. Schubert, J. Cho and J. K. Kim, "Light-emitting diodes", *Kirk-Othmer Encyclopedia of Chemical Technology*, 2000, 1–20.

(62) Z. Yu, R. J. Baxley and G. T. Zhou, "EVM and achievable data rate analysis of clipped OFDM signals in visible light communication", *EURASIP Journal on Wireless Communications and Networking*, 2012, **2012**, 321.

(63) B. Inan, S. J. Lee, S. Randel, I. Neokosmidis, A. M. Koonen and J. W. Walewski, "Impact of LED nonlinearity on discrete multitone modulation", *Journal of Optical Communications and Networking*, 2009, **1**, 439–451.

(64) I. Neokosmidis, T. Kamalakis, J. W. Walewski, B. Inan and T. Sphicopoulos, "Impact of nonlinear LED transfer function on discrete multitone modulation: Analytical approach", *Journal of Lightwave technology*, 2009, **27**, 4970–4978.

(65) T. Kamalakis, J. W. Walewski and G. Mileounis, "Empirical Volterra-series modeling of commercial light-emitting diodes", *Journal of Lightwave Technology*, 2011, **29**, 2146–2155.

(66) W. Bosch and G. Gatti, "Measurement and simulation of memory effects in predistortion linearizers", *IEEE Transactions on Microwave Theory and Techniques*, 1989, **37**, 1885–1890.

(67) M. Schetzen, "The Volterra and Wiener theories of nonlinear systems", 1980.

(68) S. A. Maas, *Nonlinear microwave and RF circuits*, Artech House, 2003.

(69) I. W. Hunter and M. J. Korenberg, "The identification of nonlinear biological systems: Wiener and Hammerstein cascade models", *Biological cybernetics*, 1986, **55**, 135–144.

(70) M. Schetzen, "Nonlinear system modeling based on the Wiener theory", *Proceedings of the IEEE*, 1981, **69**, 1557–1573.

(71) A. Garulli, L. Giarre, G. Zappa et al., "Identification of approximated Hammerstein models in a worst-case setting", *IEEE Transactions on Automatic Control*, 2002, **47**, 2046–2050.

(72) J. Kim and K. Konstantinou, "Digital predistortion of wideband signals based on power amplifier model with memory", *Electronics Letters*, 2001, **37**, 1417–1418.

(73) S. Haykin, "Adaptive filters", *Signal Processing Magazine*, 1999, **6**, 1.

(74) P. S. Chang and A. N. Willson, "Analysis of conjugate gradient algorithms for adaptive filtering", *IEEE Transactions on Signal Processing*, 2000, **48**, 409–418.

(75) I. S. Reed, J. D. Mallett and L. E. Brennan, "Rapid convergence rate in adaptive arrays", *IEEE Transactions on Aerospace and Electronic Systems*, 1974, 853–863.

(76) R. Raich and G. T. Zhou, "Orthogonal polynomials for complex Gaussian processes", *IEEE transactions on signal processing*, 2004, **52**, 2788–2797.

(77) J. Zhang, J. Yu, N. Chi and H.-C. Chien, "Time-domain digital pre-equalization for band-limited signals based on receiver-side adaptive equalizers", *Optics express*, 2014, **22**, 20515–20529.

(78) Z. Dong, X. Li, J. Yu, Z. Cao and N. Chi, "8, *times*,9.95-Gb/s Ultra-Dense WDM-PON on a 12.5-GHz Grid With Digital Pre-Equalization", *IEEE Photonics Technology Letters*, Jan. 2013, **25**, 194–197.

(79) P. Varahram, S. Jamuar, S. Mohammady and M. Hamidon, "Power amplifiers linearization based on digital predistortion with memory effects used in CDMA applications", *Circuit Theory and Design, 2007. ECCTD 2007. 18th European Conference on*, 2007, 488–491.

(80) J. K. Cavers, "Amplifier linearization using a digital predistorter with fast adaptation and low memory requirements", *IEEE transactions on vehicular technology*, 1990, **39**, 374–382.

(81) S. Choi, E.-R. Jeong and Y. H. Lee, "Adaptive predistortion with direct learning based on piecewise linear approximation of amplifier nonlinearity", *IEEE Journal of selected topics in signal processing*, 2009, **3**, 397–404.

(82) M. Djamai, S. Bachir and C. Duvanaud, "Kalman filtering algorithm for on-line memory polynomial predistortion", *Microwave Conference, 2008. EuMC 2008. 38th European*, 2008, 575–578.

(83) E. Aschbacher and M. Rupp, "Modelling and identification of a nonlinear power-amplifier with memory for nonlinear digital adaptive pre-distortion", *Signal Processing Advances in Wireless Communications, 2003. SPAWC 2003. 4th IEEE Workshop on*, 2003, 658–662.

(84) R. Gupta, S. Ahmad, R. Ludwig and J. McNeill, "Adaptive digital baseband predistortion for RF power amplifier linearization", *High Frequency Electronics*, 2006, **5**, 16–25.

(85) H. Paaso and A. Mammela, "Comparison of direct learning and indirect learning predistortion architectures", *Wireless Communication Systems. 2008. ISWCS'08. IEEE International Symposium on*, 2008, 309–313.

(86) Y. Ma, S. He, Y. Akaiwa and Y. Yamao, "An open-loop digital predistorter based on memory polynomial inverses for linearization of RF power amplifier", *International Journal of RF and Microwave Computer-Aided Engineering*, 2011, **21**, 589–595.

(87) Y. Ma, Y. Akaiwa and Y. Yamao, "Fast baseband polynomial inverse algorithm for nonlinear system compensation", *Vehicular Technology Conference (VTC Spring), 2012 IEEE 75th*, 2012, 1–5.

(88) Y. Hong, J. Chen, Z. Wang and C. Yu, "Performance of a precoding MIMO system for decentralized multiuser indoor visible light communications", *IEEE Photonics journal*, 2013, **5**, 7800211–7800211.

(89) M. Wolf, S. A. Cheema, M. A. Khalighi and S. Long, "Transmission schemes for visible light communications in multipath environments", *Transparent Optical Networks (ICTON), 2015 17th International Conference on*, 2015, 1–7.

(90) M.-A. Khalighi, S. Long, S. Bourennane and Z. Ghassemlooy, "PAM-and CAP-Based Transmission Schemes for Visible-Light Communications", *IEEE Access*, 2017, **5**, 27002–27013.

(91) X. Li, R. Mardling and J. Armstrong, "Channel capacity of IM/DD optical communication systems and of ACO-OFDM", *Communications, 2007. ICC'07. IEEE International Conference on*, 2007, 2128–2133.

(92) J. Armstrong, B. J. Schmidt, D. Kalra, H. A. Suraweera and A. J. Lowery, "SPC07-4: Performance of asymmetrically clipped optical OFDM in AWGN for an intensity modulated direct detection system", *Global Telecommunications Conference, 2006. GLOBECOM'06. IEEE*, 2006, 1–5.

(93) C.-c. Hsieh and D.-s. Shiu, "Single carrier modulation with frequency domain equalization for intensity modulation-direct detection channels with intersymbol interference", *Personal, Indoor and Mobile Radio Communications, 2006 IEEE 17th International Symposium on*, 2006, 1–5.

(94) H. Elgala, Ph.D. Thesis, Jacobs University Bremen, 2010.

(95) S. D. Dissanayake and J. Armstrong, "Comparison of aco-ofdm, dco-ofdm and ado-ofdm in im/dd systems", *Journal of lightwave technology*, 2013, **31**, 1063–1072.

(96) S. Dimitrov, S. Sinanovic and H. Haas, "Signal shaping and modulation for optical wireless communication", *Journal of lightwave technology*, 2012, **30**, 1319–1328.

(97) J. M. Kahn and J. R. Barry, "Wireless infrared communications", *Proceedings of the IEEE*, 1997, **85**, 265–298.

(98) A. Gangwar and M. Bhardwaj, "An overview: Peak to average power ratio in OFDM system & its effect", *International Journal of Communication and Computer Technologies*, 2012, **1**, 22–25.

(99) V. A. Bohara and S. H. Ting, "Theoretical analysis of OFDM signals in nonlinear polynomial models", *Information, Communications & Signal Processing, 2007 6th International Conference on*, 2007, 1–5.

(100) M. C. Dakhli, R. Zayani and R. Bouallegue, "A theoretical characterization and compensation of nonlinear distortion effects and performance analysis using polynomial model in MIMO OFDM systems under Rayleigh fading channel", *Computers and Communications (ISCC), 2013 IEEE Symposium on*, 2013, 000583–000587.

(101) M. Khalighi, S. Long, S. Bourennane and Z. Ghassemlooy, "PAM- and CAP-Based Transmission Schemes for Visible-Light Communications", *IEEE Access*, 2017, **5**, 27002–27013.

(102) "https://www.arduino.cc/documents/datasheets/LEDRGB-L-154A4SURK .pdf".

(103) L. Ding, G. T. Zhou, D. R. Morgan, Z. Ma, J. S. Kenney, J. Kim and C. R. Giardina, "A robust digital baseband predistorter constructed using memory polynomials", *IEEE Transactions on communications*, 2004, **52**, 159–165.

(104) W. Kang and S. Hranilovic, "Power reduction techniques for multiple-subcarrier modulated diffuse wireless optical channels.", *IEEE Trans. Communications*, 2008, **56**, 279–288.

(105) R. Mesleh, H. Elgala and H. Haas, "LED nonlinearity mitigation techniques in optical wireless OFDM communication systems", *Journal of Optical Communications and Networking*, 2012, **4**, 865–875.

(106) D. Zhou and V. E. DeBrunner, "Novel adaptive nonlinear predistorters based on the direct learning algorithm", *IEEE transactions on signal processing*, 2007, **55**, 120–133.

(107) H. Elgala, R. Mesleh and H. Haas, "Non-linearity effects and predistortion in optical OFDM wireless transmission using LEDs", *International Journal of Ultra Wideband Communications and Systems*, 2009, **1**, 143–150.

(108) J. K. Kim, K. Hyun and S. K. Park, "Adaptive predistorter using NLMS algorithm for nonlinear compensation in visible-light communication system", *Electronics Letters*, 2014, **50**, 1457–1459.

(109) H. Qian, S. Yao, S. Cai and T. Zhou, "Adaptive Postdistortion for Nonlinear LEDs in Visible Light Communications", *Photonics Journal, IEEE*, Aug. 2014, **6**, 1–8.

(110) R. Raich, H. Qian and G. Zhou, "Orthogonal polynomials for power amplifier modeling and predistorter design", *Vehicular Technology, IEEE Transactions on*, Sept. 2004, **53**, 1468–1479.

(111) R. B. Smith, "Two theorems on inverses of finite segments of the generalized Hilbert matrix", *Mathematical Tables and Other Aids to Computation*, 1959, **13**, 41–43.

(112) I. Neokosmidis, T. Kamalakis, J. Walewski, B. Inan and T. Sphicopoulos, "Impact of Nonlinear LED Transfer Function on Discrete Multitone Modulation: Analytical Approach", *Lightwave Technology, Journal of*, Nov. 2009, **27**, 4970–4978.

(113) E. Meijering, "A chronology of interpolation: from ancient astronomy to modern signal and image processing", *Proceedings of the IEEE*, 2002, **90**, 319–342.

(114) "https://www.kingbrightusa.com/images/catalog/spec/wp154a4sureqbfzgw.pdf".

(115) E. Eskinat, S. H. Johnson and W. L. Luyben, "Use of Hammerstein models in identification of nonlinear systems", *AIChE Journal*, 1991, **37**, 255–268.

(116) Y. Hong, J. Chen, Z. Wang and C. Yu, "Performance of a precoding MIMO system for decentralized multiuser indoor visible light communications", *IEEE Photonics Journal*, 2013, **5**, 7800211–7800211.

(117) N. Saha, R. K. Mondal, N. T. Le and Y. M. Jang, "Mitigation of interference using OFDM in visible light communication", *ICT Convergence (ICTC), 2012 International Conference on*, 2012, 159–162.

(118) W. Zhao, Q. Guo, J. Tong, J. Xi, Y. Yu, P. Niu and X. Sun, "Orthogonal polynomial-based nonlinearity modeling and mitigation for LED communications", *IEEE Photonics Journal*, 2016, **8**, 1–12.

(119) N. Saha, R. K. Mondal, N. T. Le and Y. M. Jang, "Mitigation of interference using OFDM in visible light communication", *ICT Convergence (ICTC), 2012 International Conference on*, 2012, 159–162.

(120) Z. Wang, Q. Wang, S. Chen and L. Hanzo, "An adaptive scaling and biasing scheme for OFDM-based visible light communication systems", *Optics express*, 2014, **22**, 12707–12715.

(121) L. Grobe and K.-D. Langer, "Block-based PAM with frequency domain equalization in visible light communications", *Globecom Workshops (GC Wkshps), 2013 IEEE*, 2013, 1070–1075.

(122) M. Wolf, S. A. Cheema, M. A. Khalighi and S. Long, "Transmission schemes for visible light communications in multipath environments", *2015 17th International Conference on Transparent Optical Networks (ICTON)*, July 2015, 1–7.

(123) M. A. Khalighi, S. Long, S. Bourennane and Z. Ghassemlooy, "PAM- and CAP-Based Transmission Schemes for Visible-Light Communications", *IEEE Access*, 2017, **5**, 27002–27013.

(124) Z. Ghassemlooy, W. Popoola and S. Rajbhandari, *Optical wireless communications: system and channel modelling with Matlab®*, CRC press, 2012.

(125) C. R. Lomba, R. T. Valadas and A. de Oliveira Duarte, "Efficient simulation of the impulse response of the indoor wireless optical channel", *International Journal of Communication Systems*, 2000, **13**, 537–549.

(126) C. R. Lomba, T̃. Valadas and A. de Oliveira Duarte, "Propagation losses and impulse response of the indoor optical channel: A simulation package", *International Zurich seminar on Digital communications*, 1994, 285–297.

(127) J. R. Barry, J. M. Kahn, W. J. Krause, E. A. Lee and D. G. Messerschmitt, "Simulation of multipath impulse response for indoor wireless optical channels", *IEEE journal on selected areas in communications*, 1993, **11**, 367–379.

(128) E. Eskinat, S. H. Johnson and W. L. Luyben, "Use of Hammerstein models in identification of nonlinear systems", *AIChE Journal*, 1991, **37**, 255–268.

(129) Y. Ma, S. He, Y. Akaiwa and Y. Yamao, "An open-loop digital predistorter based on memory polynomial inverses for linearization of RF power amplifier", *International Journal of RF and Microwave Computer-Aided Engineering*, 2011, **21**, 589–595.

(130) M. G. Kendall, A. Stuart and J. K. Ord, *The advanced theory of statistics*, JSTOR, 1948, vol. 1.

(131) H. Elgala, R. Mesleh and H. Haas, "Predistortion in optical wireless transmission using OFDM", *Hybrid Intelligent Systems, 2009. HIS'09. Ninth International Conference on*, 2009, **2**, 184–189.